Phytopathology® • 2023 • 113:1729-1744 • https://doi.org/10.1094/PHYTO-12-22-0465-V

Virology

Diversity and Pathobiology of an Ilarvirus Unexpectedly Detected in Diverse Plants and Global Sequencing Data

Mark Paul Selda Rivarez,[1,†] Chantal Faure,[2] Laurence Svanella-Dumas,[2] Anja Pecman,[1] Magda Tušek-Žnidaric,[1] Deborah Schönegger,[2] Kris De Jonghe,[3] Arnaud Blouin,[4] David A. Rasmussen,[5] Sebastien Massart,[4] Maja Ravnikar,[1] Denis Kutnjak,[1] Armelle Marais,[2] and Thierry Candresse[2,†]

[1] Department of Biotechnology and Systems Biology, National Institute of Biology, Ljubljana, 1000, Slovenia
[2] University of Bordeaux, INRAE, UMR 1332 Biologie du Fruit et Pathologie, Villenave d'Ornon, 33882, France
[3] Plant Sciences Unit, Flanders Research Institute for Agriculture, Fisheries and Food, Merelbeke, 9820, Belgium
[4] Plant Pathology Laboratory, TERRA-Gembloux Agro-Bio Tech, University of Liège, Gembloux, 5030, Belgium
[5] Department of Entomology and Plant Pathology, North Carolina State University, Raleigh, 27606, U.S.A.
Accepted for publication 26 June 2023.

Abstract

High-throughput sequencing (HTS) and sequence mining tools revolutionized virus detection and discovery in recent years, and implementing them with classical plant virology techniques results in a powerful approach to characterize viruses. An example of a virus discovered through HTS is Solanum nigrum ilarvirus 1 (SnIV1) (*Bromoviridae*), which was recently reported in various solanaceous plants from France, Slovenia, Greece, and South Africa. It was likewise detected in grapevines (*Vitaceae*) and several *Fabaceae* and *Rosaceae* plant species. Such a diverse set of source organisms is atypical for ilarviruses, thus warranting further investigation. In this study, modern and classical virological tools were combined to accelerate the characterization of SnIV1. Through HTS-based virome surveys, mining of sequence read archive datasets, and a literature search, SnIV1 was further identified from diverse plant and non-plant sources globally. SnIV1 isolates showed relatively low variability compared with other phylogenetically related ilarviruses. Phylogenetic analyses showed a distinct basal clade of isolates from Europe, whereas the rest formed clades of mixed geographic origin. Furthermore, systemic infection of SnIV1 in *Solanum villosum* and its mechanical and graft transmissibility to solanaceous species were demonstrated. Near-identical SnIV1 genomes from the inoculum (*S. villosum*) and inoculated *Nicotiana benthamiana* were sequenced, thus partially fulfilling Koch's postulates. SnIV1 was shown to be seed-transmitted and potentially pollen-borne, has spherical virions, and possibly induces histopathological changes in infected *N. benthamiana* leaf tissues. Overall, this study provides information to better understand the diversity, global presence, and pathobiology of SnIV1; however, its possible emergence as a destructive pathogen remains uncertain.

Keywords: histopathology, *Ilarvirus*, phylogenetics, pollen, Serratus, *Solanaceae*, symptomatology, virion morphology, virus diversity, virus transmission

†Corresponding authors: M. P. S. Rivarez; mpsrivarez@gmail.com, and T. Candresse; thierry.candresse@inrae.fr

Current address for M. P. S. Rivarez: Department of Entomology and Plant Pathology, North Carolina State University, Raleigh, 27606, U.S.A.; and College of Agriculture and Agri-Industries, Caraga State University, Butuan City, 8600, Philippines.

Current address for A. Blouin: Plant Protection Department, Agroscope, Nyon, 1260, Switzerland.

Author contributions: T.C., A.M., S.M., M.R., and D.K. were all involved in funding acquisition for the INEXTVIR project. T.C., A.M., M.R., D.K., and M.P.S.R. formulated and designed the study. T.C. supervised the study. M.P.S.R. did the majority of the experimental work and the data analyses and wrote the first draft of the manuscript. T.C. contributed to sequence database mining and genome assembly. C.F., A.M., and L.S.D. contributed to collection and transmission experiments and RT-PCR testing of samples from France and assisted in greenhouse experiments. A.P. contributed to transmission experiments and nanopore sequencing and analyses. M.T.-Ž. did the light and transmission electron microscopy experiments. D.S., S.M., K.D.J., and A.B. contributed SnIV1 sequences, and K.D.J. confirmed the detection of SnIV1 in Belgium by RT-PCR. D.A.R. helped in the conduct and interpretation of the phylogeographic analysis. All authors agreed on and significantly contributed to editing the final manuscript.

e-Xtra: Supplementary material is available online.

The author(s) declare no conflict of interest.

The combination of classical virology techniques, modern high-throughput sequencing (HTS), and bioinformatics tools provides a powerful approach to detect, identify, and characterize viruses and monitor changes in their populations even before they emerge and cause disease outbreaks (Kumar et al. 2022; Maclot et al. 2020; McLeish et al. 2021). The COVID-19 pandemic and the persistent risks posed by plant and animal virus diseases to our food supply (Meurens et al. 2021; Morens et al. 2020; Ristaino et al. 2021) have increased interest in viromic surveys of ecosystems and data-driven virus discovery (Carroll et al. 2018; Lauber and Seitz 2022). This led to a recent surge in the discovery of viruses and other virus- or viroid-like agents from various studies (Edgar et al. 2022; Gregory et al. 2019; Hou et al. 2023; Lee et al. 2023; Mifsud et al. 2022; Neri et al. 2022; Rivarez et al. 2023; Zayed et al. 2022). As a result, hundreds of thousands of putative novel viruses remain uncharacterized due to the astounding amount of experimental work

Funding: Support for this work was mainly provided by the Horizon 2020 Marie Skłodowska-Curie Actions Innovative Training Network (H2020 MSCA-ITN) project "Innovative Network for Next Generation Training and Sequencing of Virome (INEXTVIR)" (grant GA 813542) under the management of the European Commission-Research Executive Agency and the Administration of the Republic of Slovenia for Food Safety, Veterinary Sector and Plant Protection and Slovenian Research Agency (grants P4-0165, P4-0407, and J4-4553). Support in Belgium was provided by the Belgian FPS Health Food Chain Safety and Environment (Project RT18/3 SEVIPLANT). M. P. S. Rivarez received funding from the Department of Science and Technology–Philippine Council for Agriculture, Aquatic, and Natural Resources Research and Development (DOST–PCAARRD) of the Republic of the Philippines (Balik Scientist Program [Republic Act 11035]).

this requires. For plant virologists, this entails the immense task of uncovering the biological properties of newly identified plant viruses and systematically assessing their possible economic and biosecurity risks (Fontdevila et al. 2023; Hou et al. 2020; Massart et al. 2017; Rivarez et al. 2021).

Some recent studies combined classical and modern tools and techniques to characterize recently discovered plant viruses. For instance, the biological characterization of an emerging pathogen of tomato, Physostegia chlorotic mottle alphanucleorhabdovirus (family *Rhabdoviridae*), was significantly accelerated through an international collaboration driven by HTS data (Temple et al. 2022, 2023). Recently, mining of thousands of *Arabidopsis thaliana* publicly available sequence read archive (SRA) datasets uncovered a novel comovirus (family *Secoviridae*), Arabidopsis latent virus 1, which was demonstrated to be mechanically and seed transmitted but causes no symptoms in *A. thaliana* (Verhoeven et al. 2023). A recent study on *Prunus*-associated luteoviruses (family *Luteoviridae*) also uncovered a new luteovirus through a search of SRA datasets (Khalili et al. 2023). Many HTS-based discoveries of crop and non-crop viruses have also been reported (Gaafar et al. 2020; Ma et al. 2019; Rivarez et al. 2023; Xu et al. 2017), but only a small subset of these studies has biologically characterized the identified viruses (Hou et al. 2020; Rivarez et al. 2021).

Among these newly discovered but marginally characterized viruses is Solanum nigrum ilarvirus 1 (SnIV1), which was recently associated with wild, weedy, or cultivated species, primarily from the *Solanaceae* family. SnIV1 belongs to the genus *Ilarvirus*, which is the largest genus in the family *Bromoviridae*, with 22 recognized species (ICTV 2023), some causing significant economic losses (Rivarez et al. 2021). Ilarviruses are known to be pollen and/or seed transmitted (Card et al. 2007; Mink 1993), and their transmission was also reported to be facilitated by thrips or pollinators (Bristow and Martin 1999). Ilarviruses pose persistent threats to fruit production, such as for *Prunus* species (Pallas et al. 2012) or blackberry (*Rubus fruticosus*) (Poudel et al. 2014). In recent years, several ilarviruses were reported to cause problems in tomato in the United States, including tomato necrotic streak virus (Adkins et al. 2015; Badillo-Vargas et al. 2016) and tomato necrotic spot virus (Bratsch et al. 2018, 2019). Other economically important ilarviruses known to be emerging or endemic pathogens of tomato include parietaria mottle virus (PMoV) (Aparicio et al. 2018), tobacco streak virus (TSV) (Sharman et al. 2015), and spinach latent virus (Vargas-Asencio et al. 2013). TSV and PMoV are the closest phylogenetically related viruses to SnIV1 (Ma et al. 2020).

SnIV1 was detected in *Solanaceae* crop and non-crop plants from France (*S. nigrum* and *S. lycopersicum*) (Ma et al. 2020), Slovenia (*Physalis* sp.) (Rivarez et al. 2023), South Africa (*S. chenopodioides*) (Mahlanza et al. 2022), and Greece (*Capsicum annuum*) (Orfanidou et al. 2022). A recent report from Greece demonstrated SnIV1 infectivity in *N. benthamiana* and *C. annuum* (Orfanidou et al. 2022). However, SnIV1 infectivity has not yet been extensively tested for the other crops and wild plants with which it has been found to be associated. Interestingly, SnIV1 was concurrently reported under different names (i.e., grapevine-associated ilarvirus, surrounding legume-associated ilarvirus, and Erysiphe necator-associated ilar-like virus 1) in viromic studies involving plants from different botanical families. These studies detected SnIV1 sequences in association with legume (*Fabaceae*) plants from Germany (Gaafar et al. 2020) and grapevines (*Vitaceae*) from Italy and Spain (Chiapello et al. 2019, 2020). Recently, SnIV1 has also been reported from *Rosaceae* fruit trees, such as peaches (*Prunus persica*) from the United States (Dias et al. 2022) and apricots (*Prunus armeniaca*) from South Africa (Bester and Maree 2023). Such a diverse list of source materials and potential hosts is unusual for an ilarvirus because genus members usually have host ranges limited to species of the same botanical family (Badillo-Vargas et al. 2016).

In this study, aside from modern HTS and sequence mining approaches, classical techniques such as experimental host range tests, extensive geographical surveys, histopathological observations, diversity and phylogenetic analyses, and subsequent virus detection using RT-PCR tests were implemented to characterize SnIV1. The general aim was to assess its global diversity and distribution and to characterize some of its biological properties. Specifically, we aimed to answer the following questions: (i) Can information on SnIV1 geographic distribution and tentative hosts be expanded using an HTS-based viromic survey of various plant species and by searching relevant SRA datasets? (ii) Do global isolates of SnIV1 show distinct phylogenetic clustering, and what is the SnIV1 level of genetic diversity compared with that of other related species, such as TSV and PMoV? (iii) Can SnIV1 infect a range of experimental host plants and induce histopathological changes in these hosts? (iv) What are the potential routes of transmission of SnIV1? Collectively, the data gathered from this study contribute to a better understanding of the diversity and pathobiology of this little-known ilarvirus, which should aid in assessment of its risk and further spread and emergence as a destructive pathogen.

Materials and Methods

This study was a collaborative effort involving several European partners. The majority of the experiments, including SRA mining, inoculation, and other greenhouse experiments, were done at INRAE, whereas additional inoculation experiments, nanopore sequencing, and electron microscopy were done at NIB. Separate HTS-based surveys with PCR confirmation were performed at ULiege and ILVO. The shared aim was to consolidate information on the detections of SnIV1, share genomic sequences for further analyses, and perform further biological and epidemiological characterization.

Plant samples

The following plant species were collected in the INRAE Bordeaux research center (Villenave d'Ornon, France), tested for SnIV1 infection, and/or sequenced in the surveys of this study: (i) *S. villosum* that underwent Nanopore sequencing and RT-PCR testing, (ii) *S. nigrum* that underwent RT-PCR testing, (iii) *Vitis vinifera* 'Sauvignon', (iv) *V. vinifera* 'Ugni Blanc', and (v) *Daucus carota* subsp. *carota* that underwent Illumina sequencing and RT-PCR testing. Samples of *S. melongena* and *S. tuberosum* were similarly obtained from selected farms in Belgium, were submitted for Illumina sequencing, and underwent further RT-PCR testing. Details on how RNA was extracted and sequenced are presented below.

Following positive RT-PCR tests for SnIV1, two *S. villosum* plants were uprooted from the field, cleaned, pruned, and introduced in an insect-proof greenhouse. Two SnIV1-positive grapevine samples (*V. vinifera* 'Sauvignon') were introduced in the same greenhouse by preparing and transplanting cleaned stem cuttings from each plant. Both samples were maintained for 3 months in the greenhouse before retesting them for SnIV1 and utilizing them in subsequent experiments as described below.

Nucleic acid extraction methods for RT-PCR assays and Illumina-based HTS

Different methods were used for RNA extraction from field samples, greenhouse-introduced plants, and inoculated test plants prior to RT-PCR testing and/or HTS on Illumina platforms.

For total RNA extractions performed in France, a previously described method (Foissac et al. 2005) was used for leaves, stems, seeds, fruits, roots, pollen, and floral parts of *S. villosum* and for the pollen of *S. nigrum* prior to RT-PCR testing. Likewise, this protocol was used to extract total RNA individually from inoculated test plants prior to RT-PCR testing. The Spectrum Total Plant RNA kit (Sigma-Aldrich, France) was used, following the kit instruc-

tions, to extract total RNA from grapevine leaves, petioles, bark, and phloem scrapings for RT-PCR testing. A previously described total RNA extraction protocol (Svanella-Dumas et al. 2022) was used for individual grapevine leaf tissues (for cultivar Ugni Blanc) or phloem scrapings (cultivar Sauvignon) prior to HTS. Double-stranded RNA (dsRNA) from 45 pools of carrot plants (50 plants each) was purified according to a previously described protocol (Ma et al. 2020) prior to HTS (Schönegger 2023).

Virion-associated nucleic acid (VANA) was purified from pools of 50 individual samples each for *S. melongena* and *S. tuberosum* from Belgium prior to HTS as previously described (Hammond et al. 2020; Palanga et al. 2016).

Prior to RT-PCR assays of inoculated test plants from Slovenia, the RNeasy Plant Mini Kit (Qiagen, U.S.A.) was used to extract total RNA from all samples following the kit instructions.

RT-PCR assays

Oligonucleotide primers specific for SnIV1 RNA 3 segment or tomato betanucleorhabdovirus 2 (TBRV2, detected in mixed infection with SnIV1 in *S. villosum*) (Supplementary Table S1) were used in RT-PCR tests conducted in Slovenia using the OneStep RT-PCR kit (Qiagen) as previously described (Rivarez et al. 2023). Additional SnIV1 primers targeting RNA 1 and RNA 3 segments were designed using OligoCalc (Kibbe 2007) and used in two-step RT-PCR reactions as previously described (Marais et al. 2014) to test for SnIV1 in different plant samples from France. In each RT-PCR assay, RNA extracts from SnlV1-positive samples were used as positive controls, RNA extraction controls and/or healthy plants as negative controls, and no template (water only) as a blank control.

Nanopore sequencing

A CTAB-based protocol (Chang et al. 1993) was used to extract total RNA from SnIV1-infected *S. villosum* that served as inoculum and from inoculated *N. benthamiana* prior to nanopore sequencing. Details of the nanopore sequencing methods can be found in the Supplementary Material.

Search for SnIV1 sequences in databases and the literature and assembly of SnIV1 genomes

Publicly available databases and the literature were searched for SnIV1 sequences, and a previously described bioinformatic pipeline was used for the reference-guided assembly of SnIV1 genomes from HTS data in this study (Pecman et al. 2017; Rivarez et al. 2023). Details of the methods used can be found in the Supplementary Material.

Multiple sequence alignments and recombination detection analyses

To examine the molecular diversity of SnIV1, nucleotide (nt) sequences were aligned using MUSCLE (Edgar 2004) as implemented in MEGA X (Kumar et al. 2018). To compare SnIV1 diversity with that of other phylogenetically related ilarviruses, sequences of isolates of TSV and PMoV were retrieved from GenBank r.v. 250 and similarly aligned.

Prior to diversity and phylogenetic analyses, possible recombination events among the SnIV1, TSV, or PMoV sequences were checked using RDP v. 5 (Martin et al. 2021). A recombination event was considered significant if it had a *P* value less than 10^{-4} in at least four of the methods used (RDP, GENECONV, Bootscan, Maxchi, Chimaera, SiSscan, PhylPro, LARD, 3Seq) (de Klerk et al. 2022; Stewart et al. 2014). Recombinant sequences were removed, and unaligned ends for each genome segment of the remaining isolates were manually trimmed.

Nucleotide diversity and genetic variation analyses

The coding regions of the three RNA segments of SnIV1, TSV, and PMoV were used for subsequent diversity and genetic variation analyses. The movement protein (MP) and coat protein (CP) open reading frames (ORFs) from the RNA 3 segment of each viral isolate were concatenated into a contiguous sequence. Because most isolates had a full RNA 3 sequence, their MP and CP were concatenated to achieve uniformity in length and retain coding information for all isolates, which would be useful in the subsequent analyses in which nucleotide diversity was calculated in codon-based steps (i.e., step size of 3; see description below). In this way, variable regions can be easily pinpointed to specific coding regions, not just in any random portion of the genome. The RNA 1, RNA 2, and concatenated RNA 3 alignments were then used separately to perform pairwise identity and nucleotide diversity analyses. For each genome segment, pairwise identities were calculated using SDT v. 1.2 (Muhire et al. 2014).

Genome-wide polymorphisms were detected, and nucleotide diversities (pi [π]) and molecular genetic variation (theta [θ], based on π and finite sites model) (Subramanian 2016) were calculated with DnaSP v. 6 (Rozas et al. 2017) using a sliding window of 30 bases and a step size of 3. Overall genetic distances were calculated in MEGA X (Kumar et al. 2018) using the same set of alignments. Overall π is the average probability of observing nucleotide differences at a single locus among the sequences or isolates being compared, overall θ is a measure of the number of mutations or mutation rate among the sequences or isolates being compared, and overall genetic distance is the average of all pairwise genetic distances among the sequences or isolates being compared.

Phylogenetic analyses

Maximum likelihood phylogenetic analyses were used to examine the clustering of SnIV1 isolates from diverse sources. The multiple sequence alignments described above were used as input for the analyses performed in MEGA X (Kumar et al. 2018). The most suitable substitution model was selected based on the Bayesian information criterion, and the analyses were performed with 1,000 bootstrap replicates. iToL v. 6.4 (Letunic and Bork 2021) was used to visualize and annotate the resulting phylogenetic trees. Bayesian phylogeographic analysis was done in BEAST v. 2.7.4 (Bouckaert et al. 2019), as described in detail in the Supplementary Material.

Disinfection of plant tissues and seeds

To remove possible surface contaminants, including pollen grains possibly carrying SnIV1, plant tissues (including seeds) were surface disinfected prior to RNA extraction. This was done on plant samples from INRAE, France, including the greenhouse-introduced *S. villosum* and grapevine (cultivar Sauvignon) tissues, as well as leaves of inoculated test plants. Disinfection was done by soaking the tissues in a 5% sodium hypochlorite solution for 10 min with intermittent agitation, followed by six washes in sterile water with blot-drying in between. The sodium hypochlorite solution and water were replaced for every new tissue fragment being disinfected and washed. After the washing, disinfected plant tissues were air-dried for at least 15 min before proceeding with RNA extraction.

Preparation of floral parts and pollen for RNA extraction

Individual floral parts and pollen were tested for the presence of SnIV1. Ten flowers from the greenhouse-introduced, SnIV1-infected *S. villosum* plant (described above) were collected. Pedicels, sepals, pistils, stamens, and petals were dissected and separately pooled prior to RNA extraction.

Pollen grains were collected from the same *S. villosum* plant described above and from *S. nigrum* inoculated by approach grafting (see details below). Briefly, ripe stamens were separated from flowers and vortexed in sterile water to liberate and suspend pollen grains. Stamens were then removed, and the purity and integrity of pollen grains were verified under an Eclipse Ni-U (Nikon, Japan) microscope with a dark field condenser in reflection mode. Pollen grains suspended in sterile water were briefly ground using a sterile

plastic pestle suitable for 1.5-ml Eppendorf tubes before proceeding with RNA extraction.

Mechanical transmission tests

The greenhouse-introduced SnIV1-infected *S. villosum* was used as the inoculum source for the mechanical inoculations. Twenty individuals per plant species with three plants for each species kept as mock-inoculated controls were used as test plants. The inoculum was prepared by homogenizing 1.0 g of infected tissue with 10 ml of phosphate buffer (0.02 M, pH 7.8, supplemented with 0.112 g of sodium diethyldithiocarbamate trihydrate [DIECA] and 0.649 ml of β-mercaptoethanol per 100 ml of total volume). Activated charcoal powder (0.1 g per 10 ml of inoculum) was added to the ice-cold inoculum, which was then used to rub-inoculate plants using approximately 0.1 ml of inoculum on the second and third youngest leaves of plants that were dusted with carborundum. Plants were maintained in an insect-proof greenhouse with the temperature set at 20 to 24°C, with a 16/8 h day/night cycle. Samples from individual plants or pooled equal amounts of uninoculated newly formed leaves from inoculated plants were tested for SnIV1 presence, up until 35 days postinoculation (dpi).

Graft transmission tests

The greenhouse-introduced, SnIV1-infected *S. villosum* was used in approach-grafting transmission experiments by using the healthy, greenhouse-grown *S. nigrum* plants as recipients ($n = 3$). Briefly, about a 2- to 3-cm vertical length of the epidermal-parenchymal layer was removed on one side of a young stem in both source and recipient plants. The exposed tissues were joined together and secured with a perforated adhesive tape.

For chip bud grafting, the same infected *S. villosum* plant was used to obtain 2- to 3-cm superficial tissue strip pieces from a young stem that were joined with the exposed internal tissues of a young stem of recipient *S. nigrum* plants ($n = 2$). The joined tissues were again secured with perforated adhesive tape. Both approach- and chip bud-grafted plants were maintained in a greenhouse kept at 20 to 24°C, with a 16/8 h day/night cycle, before RT-PCR testing for SnIV1 at 5 weeks after grafting.

Seed transmission tests

Seeds were collected from a greenhouse-introduced SnIV1-infected *S. villosum* ($n = 73$) and from two randomly selected *S. nigrum* and two *S. villosum* plants from the field (INRAE, Bordeaux, France) and surface disinfected as described above. A subsample of these seeds was also tested by RT-PCR to confirm SnIV1 infection prior to sowing. Seeds were sown in a soil tray and maintained in the greenhouse, with conditions set at 20 to 24°C, with a 16/8 h day/night cycle. RT-PCR testing of germinated seedlings for SnIV1 infection was performed at 3 and 5 weeks after sowing.

Microscopic examination of SnIV1 virions and infected leaf tissues

Leaves of the same age and size from mock-inoculated and SnIV1-infected *N. benthamiana* plants were sampled at 49 dpi. For negative staining, leaf tissue homogenates were prepared by macerating them in 1.5-ml Eppendorf tubes containing phosphate buffer (0.1 M, pH 7.0). The homogenates were applied to Formvar-coated, carbon-stabilized copper grids and negatively stained with 1% uranyl acetate (SPI Supplies, U.S.A.) in phosphate buffer (0.1 M, pH 7.0) before inspection using a Talos transmission electron microscope (TEM) (Thermo Fisher, U.S.A.).

For preparation of thin tissue sections for light microscopy, small pieces of the same leaves used for TEM observations were fixated in 3% glutaraldehyde in phosphate buffer (0.1 M, pH 7.0) for 16 h at 4°C, which was followed by post-fixation in 1% osmium tetroxide in phosphate buffer (0.1 M, pH 7.0) and embedding in Agar 100 resin (Agar Scientific, U.K.). Semi-thin sections (0.6 μm) were cut with a Reichert Ultracut S ultramicrotome (Leica, Germany), stained with Azure II/methylene blue, and observed with an Axioskop 2 Plus microscope (Carl Zeiss, Germany).

Results

SnIV1 genome sequences obtained from HTS of different plant species

SnIV1 genomes were sequenced and assembled in four different HTS experiments. Nanopore sequencing of rRNA-depleted total RNA from *S. villosum* (inoculum source) and inoculated *N. benthamiana* yielded a mean read depth or average coverage ranging from 29 to 15,841× with 100% genome coverage in all three genome segments (Table 1).

Illumina sequencing of dsRNA from wild carrots sampled in France yielded near-complete SnIV1 genome segments with an average coverage ranging between 94 and 1,218× for the three segments. Positive RT-PCR tests confirmed the presence of SnIV1 in the dsRNA extract of the pooled wild carrot samples.

HTS of a pool of five grapevine (cultivar Sauvignon) phloem scraping samples yielded 481 reads that mapped on SnIV1 genome segments. RT-PCR tests confirmed the presence of SnIV1 in two of the five grapevines. Illumina short-read sequencing of rRNA-depleted total RNA from two grapevine (cultivar Ugni Blanc) plants yielded near-complete SnIV1 genomes with average coverage of 16 to 60×. This detection was later confirmed by RT-PCR tests for both individual samples.

Illumina sequencing of VANAs from a pool of *S. melongena* and *S. tuberosum* samples collected in Belgium yielded a partial genome of SnIV1, with only a near-complete RNA 3 segment assembled from the *S. melongena* dataset. The detection of SnIV1 in pooled samples of both species was later confirmed with a positive RT-PCR test. The amplicon from *S. tuberosum* was Sanger sequenced and confirmed to be SnIV1.

RT-PCR detection of SnIV1 in different plant tissues

The presence of SnIV1 was further investigated in different tissues of SnIV1-positive *S. villosum* and grapevines (cultivar Sauvignon) that were cleaned before introduced and grown for several months in the greenhouse. Three cuttings each from the two Sauvignon grapevines were sampled for bark, phloem, petiole, and newly grown leaf tissues. All tissues tested negative for SnIV1 at 5 and 8 months post-introduction into the greenhouse (Table 2).

Disinfected tissues of one of the two asymptomatic *S. villosum* plants replanted in the greenhouse were also tested 3 months after introduction into the greenhouse. All *S. villosum* tissues that were surface disinfected and tested in pools (i.e., leaf, stem, fruits, root, flowers, and seeds pools), as well as non-disinfected individual floral parts and pollen, tested positive for SnIV1. However, because the individual floral parts were not disinfected and ensured to be free from pollens, detection of SnIV1 might reflect presence of the virus in these floral parts or, alternatively, presence of contaminated pollen grains.

The presence of SnIV1 was also evaluated in pollen from a graft-inoculated *S. nigrum* plant (see details below) maintained in the greenhouse and in seeds from randomly sampled wild *S. nigrum* and *S. villosum* collected from the INRAE Bordeaux research center. Pollen collected from the graft-inoculated *S. nigrum* plant tested positive for SnIV1. RT-PCR tests of surface-disinfected individual seeds revealed the presence of SnIV1 in seeds from only one of the two randomly sampled *S. nigrum* plants from the field, whereas seeds from two *S. villosum* plants that were similarly processed tested negative for SnIV1.

In silico detection of SnIV1 in databases and in the literature

Information on sequences and existing records of SnIV1 were collected to gain a comprehensive picture of its global diversity and geographic distribution (Table 3; Supplementary Table S2). Aside from SnIV1 genomes deposited in GenBank database r.v. 250,

SnIV1 was also detected through BLASTn homology searches in a publicly available transcriptome shotgut assembly of hop (*Humulus lupulus* var. *lupulus*, family *Cannabaceae*) from Japan (Natsume et al. 2015). So far, this is the only detection of SnIV1 sequences that are linked to samples from Asia with a dataset deposited in GenBank database. Furthermore, search of SRA datasets through palmID in Serratus (Edgar et al. 2022) returned 80 datasets with RdRp 'palmprint' sequences that were 100% identical to that of SnIV1 (103 amino acid residues, E-value $< 10^{-74}$). These results included detections of SnIV1 in sequence datasets from China, the United States, and several European countries.

A literature search identified recent studies that detected SnIV1 sequences that were not yet available in GenBank r.v. 250 at the time of writing. This search identified four new plant viromic or disease etiology studies, including two that detected the virus in South Africa, which represent the first reports of SnIV1 on the African continent (Bester and Maree 2023; Mahlanza et al. 2022). The other two studies are viromic studies of peach in the United States (Dias et al. 2022) and an HTS study of symptomatic peppers (hybrid Arlequin F1) from Greece (Orfanidou et al. 2022). The study from Greece demonstrated the mechanical transmissibility and infectivity of SnIV1 in *N. benthamiana* and in the same genotype of peppers.

In total, 25 independent studies that detected SnIV1 sequences were identified, 15 of which were gathered through the palmID search. In terms of timing, the oldest SRA dataset with SnIV1 presence was released in 2013 and is a transcriptomic study of *Medicago truncatula* root nodules from France (Roux et al. 2014),

TABLE 1. High-throughput sequencing of plant samples collected from field surveys and those collected from transmission experiments emphasizing the detection of Solanum nigrum ilarvirus 1 (SnIV1) (and tomato betanucleorhabdovirus 2 [TBRV2]) sequences and its genome assembly

Sequencing approach and reference for assembly and mapping methods	Source plant (family) and sequence read archive accession number or public repository identifier[a]	Number of quality-screened reads (min.−max. read length)[b]	SnIV1 and TBRV2 genome mapping[c]			Consensus genome GenBank accession number[d]
			Genome segment (for SnIV1)	Number of reads mapped (mean read depth or average coverage)[e]	Percent genome covered	
Nanopore sequencing of rRNA-dep totRNA[f] (Pecman et al. 2022)	*Solanum villosum**,#,g (*Solanaceae*) SRR21292491	113,093 (100−6,769 nt)	RNA 1	167 (38×)	100.0	OP561316
			RNA 2	106 (29×)	100.0	OP561317
			RNA 3	1,287 (380×)	100.0	OP561318(12)
			TBRV2	424 (21×)	100.0	OP441765
	*Nicotiana benthamiana**,#,h (*Solanaceae*) SRR21292490	183,605 (100−4,702 nt)	RNA 1	5,687 (933×)	100.0	OP561319
			RNA 2	1,449 (317×)	100.0	OP561320
			RNA 3	64,256 (15,841×)	100.0	OP561321(13)
			TBRV2	859 (31×)	100.0	OP441766
Illumina sequencing of rRNA-dep totRNA[f] (Svanella-Dumas et al. 2022)	*Vitis vinifera* 'Sauvignon'*,g (*Vitaceae*) doi:10.57745/ZIXT4A	144,803,940 (100−150 nt)	RNA 1	179 (9.6×)	72.0	(–)[i]
			RNA 2	74 (7×)	56.0	(–)
			RNA 3	228 (11.4×)	66.0	(–)
			TBRV2	(–)	(–)	(–)
	Vitis vinifera 'Ugni Blanc'*,g (*Vitaceae*) plant 1 doi:10.57745/ZIXT4A	41,648,925 (60−150 nt)	RNA 1	564 (20×)	98.6	(–)
			RNA 2	362 (16×)	97.4	(–)
			RNA 3	410 (23×)	96.6	OP561325(7)
			TBRV2	0	0	(–)
	Vitis vinifera 'Ugni Blanc'*,g (*Vitaceae*) plant 2 doi:10.57745/ZIXT4A	46,064,375 (60−150 nt)	RNA 1	900 (34×)	98.2	OP561326
			RNA 2	854 (41×)	99.0	OP561327
			RNA 3	1,008 (60×)	98.4	OP561328(6)
			TBRV2	0	0	(–)
Illumina sequencing of dsRNA[j] (Schönegger 2023)	*Daucus carota* subsp. *carota*g,k (*Apiaceae*) doi:10.57745/ZIXT4A	9,823,623 (100−114 nt)	RNA 1	5,270 (172×)	97.4	OP561322
			RNA 2	2,314 (94×)	94.7	OP561323
			RNA 3	24,549 (1,218×)	99.0	OP561324(8)
			TBRV2	0	0	(–)
Illumina sequencing of VANA[l] (Buzkan et al. 2019)	*Solanum melongena**,g,k (*Solanaceae*) SRR21292489	2,441,462 (150 nt)	RNA 1	357 (16×)	86.2	(–)
			RNA 2	70 (4×)	42.4	(–)
			RNA 3	887 (59×)	96.7	OP561329(2)
			TBRV2	0	0	(–)
	*Solanum tuberosum**,g,k (*Solanaceae*) Dataset not deposited	8,599,952 (150 nt)	RNA 1	Not assembled	(–)	(–)
			RNA 2	Not assembled	(–)	(–)
			RNA 3	54 (4×)	26.3	OP967014[m]
			TBRV2	0	0	(–)

[a] High-throughput sequencing detections confirmed by RT-PCR in individual plants are marked by an asterisk (*) for SnIV1 and hashtag (#) for TBRV2.
[b] Number of valid reads after quality screening and trimming of barcodes. The numbers in parentheses represent the range of read length in number of nucleotides.
[c] One of the SnIV1 genomes in GenBank (a.n. OL472060 to OL472062) and the TBRV2 genome (a.n. OL472116) were used in reference-based genome assembly in CLC-GWB, with at least 90% identity and coverage threshold. These genomes were also used to determine the percentage of genome (or genome segment) covered by the mapping.
[d] Accession numbers deposited in GenBank as third-party annotations (TPAs), with superscript numbers in parentheses corresponding to each SnIV1 RNA3 genome segment that was used in the phylogenetic tree construction for Figure 1 and Supplementary Figure S2.
[e] On average, number of times each locus in a reference genome is covered by the mapped reads.
[f] Ribosomal RNA-depleted total RNA.
[g] Samples collected from the field or introduced into the greenhouse.
[h] This is from a 33 dpi sample of an individual plant that was mechanically inoculated with infected tissues from greenhouse-introduced *Solanum villosum*.
[i] (–) indicates sequence was not deposited because only partial or fragmented genome was assembled or the typical open reading frames were not found, were problematic, or indicated that information is not available.
[j] Double-stranded RNA.
[k] This consists of 50 plants of the same species pooled into one composite sample, prior to dsRNA extraction.
[l] Virion-associated nucleic acid.
[m] Sequenced amplicon from the RT-PCR detection of SnIV1 in a composite *S. tuberosum* sample from Belgium.

whereas the most recent study concerns the viromic exploration of wild *Solanum* species (Mahlanza et al. 2022) and apricots (*P. armeniaca*) (Bester and Maree 2023) in South Africa. The geographic origin of the biological samples from these studies spanned five out of the six habitable continents, or 11 countries, including eight independent studies conducted in the United States. Seventeen studies involved sequencing of plant samples, including seven that involved sequencing of members of *Solanaceae* family. Of the seven studies that utilized non-plant samples, four involved the sequencing of bee species (*Apidae*). These in silico searches highlighted associations of SnIV1 with 12 different plant species of economic importance (e.g., crop, medicinal, ornamental, or fuel feedstock), six non-crop or wild plant species, and five animal species.

SnIV1 genomes assembled from global SRA datasets

SnIV1 genomic sequences were also assembled from the representative SRA datasets identified above. In this effort, only a small subset of the 80 palmID search hits were used, with the assumption that SnIV1 isolates are possibly not significantly diverse within a single study that analyzed samples collected in the same year and country by the same research team. SnIV1 genome segments were reconstructed by reference-guided assembly, yielding average coverages ranging from 4 to 77,350×. In total, 59 of the 63 genome segments (representing 21 isolates) were successfully reconstructed and deposited in GenBank.

TABLE 2. RT-PCR detection of Solanum nigrum ilarvirus 1 (SnIV1) in different tissues from greenhouse-introduced plants or from plants growing in the field

Place of collection or sample description	Plant species	Plant tissue	Number of SnIV1(+)/ number of samples tested
Greenhouse-introduced or greenhouse-grown plants	*Vitis vinifera* 'Sauvignon'[a]	Leaves (plant 1)	0/3
		Petioles (plant 1)	0/3
		Bark (plant 1)	0/3
		Phloem (plant 1)	0/3
		Leaves (plant 2)	0/3
		Petioles (plant 2)	0/3
		Bark (plant 2)	0/3
		Phloem (plant 2)	0/3
	Solanum villosum[b]	Leaves	4/4
		Stems	5/5
		Fruits	4/4
		Roots	1/1
		Flowers	1/1
		Pedicels	1/1
		Sepals	1/1
		Pistils	1/1
		Stamens	1/1
		Petals	1/1
		Seeds	8/10
		Pollen[c] (plant 1)	1/1
		Pollen[c] (plant 2)	1/1
	S. nigrum[d]	Pollen	1/1
Field (growing in the wild)	*S. nigrum*	Seeds (plant 1)	5/10
		Seeds (plant 2)	0/10
	S. villosum	Seeds (plant 1)	0/10
		Seeds (plant 2)	0/10

[a] This represents testing of cuttings from two SnIV1-positive plants introduced as eight stem cuttings each in the greenhouse and tested 4 and 8 months after transplanting.

[b] This represents results from a single SnIV1(+) plant introduced in the greenhouse and tested 3 months later. This plant also tested positive for tomato betanucleorhabdovirus 2 (TBRV2). Multiple samples from *S. villosum* represent tissues that were collected from different parts (i.e., older stems/leaves, younger stems/leaves, and so on).

[c] Pollen was collected from the two *S. villosum* plants maintained in the greenhouse and tested separately.

[d] This plant is one of the three approach-graft inoculated plants and tested positive for SnIV1.

Phylogenetic clustering and pairwise identity comparisons of SnIV1 global isolates

No recombination was detected in the alignment of concatenated MP and CP ORFs (RNA 3 segment); thus, this was used to reconstruct a maximum likelihood phylogenetic tree of the global isolates of SnIV1 (Fig. 1). Four major clades or lineages were observed, including two distinct basal lineages: one comprising four isolates from Belgium ($n = 2$, from eggplant [a.n. OP561329] and from honeybees [a.n. BK061661]), Germany ($n = 1$, from a *Fabaceae* weed [a.n. MN412727]), and Greece ($n = 1$, from pepper [a.n. OP066716]), forming a monophyletic clade with 99% bootstrap support (b.s.), and the other basal lineage consisted of a single isolate from Slovenia (from *Physalis* sp. [a.n. OL472062]). Isolates from elsewhere in the world collectively formed a poorly supported clade (60% b.s.), with the Slovenian isolate as the basal lineage. The rest of the isolates formed phylogenetic clusters of mixed country or continental origin. However, Bayesian phylogeographic analysis resulted in uniformly low probabilities for all ancestral locations near the root (Supplementary Fig. S2), reflecting a high degree of uncertainty surrounding the geographic origin of SnIV1.

In terms of percent pairwise nucleotide identity based on concatenated MP-CP ORFs (RNA 3), isolates of the basal European lineages were 94.5 to 96.6% identical to other isolates, whereas the rest of the isolates were 96.2 to 100% identical to each other (Supplementary Fig. S1). When the other genome segments were analyzed, isolates of the basal European lineage (Belgian, Greek, and German isolates only) were only 90.8 to 92.2% identical to the rest of the isolates using RNA 1 (methyltransferase-helicase [ORF 1a]) and 92.1 to 93.3% identical when using RNA 2 (RdRp and viral suppressor of RNA silencing proteins [ORFs 2a and 2b]). Likewise, patterns of phylogenetic clustering similar to that of the RNA 3 phylogenetic tree were observed in the RNA 1 and RNA 2 phylogenetic trees with the distinct basal lineage of European origin.

Diversity of SnIV1 compared with closely related ilarviruses

The recombination-free alignments of SnIV1 isolates and isolates of its two phylogenetically closest species (TSV, with a wide host range, and PMoV, with a narrow host range) were used to perform comparative diversity analyses (Fig. 2A to C). It is worthwhile to note that the number of available sequences varies among the three species. TSV has the highest number of sequences across the three genome segments, closely followed by SnIV1, whereas PMoV has the lowest number of sequences available. Inspection of π (nucleotide diversity) along the coding regions of each genome segment indicated that SnIV1 populations generally have lower π when compared with TSV, which has the highest overall π in any genome segment, even though they have a comparable number of isolates. This is obvious when examining genome-wide π for RNA 2. For TSV and PMoV, π values reach up to 27 to 37% probability of observing nucleotide differences at a single locus for any pairwise sequence comparison. However, the highest π values for any segment of SnIV1 are around 0.11 only (or 11% probability of observing single nucleotide differences). When overall π, molecular genetic diversity (θ), and overall genetic distance, were compared among the three viruses, TSV stood out with the highest values in all three segments when compared with those of both PMoV and SnIV1 (Fig. 2D).

Transmission and experimental host range of SnIV1

Approach and chip-bud grafting experiments demonstrated that SnIV1 can be transmitted through these methods from *S. villosum* to healthy *S. nigrum* plants. Newly formed leaves of plants inoculated by both grafting methods developed symptoms such as mild vein yellowing and slight leaf crinkling (Fig. 3F and G) and tested positive for SnIV1 at 18 and 27 dpi (Table 4).

Eight plant species were mechanically inoculated, seven of which are *Solanaceae* members, including two cultivars of *S. lycopersicum.* Three solanaceous species (*N. benthamiana*, *N. occiden-*

TABLE 3. Solanum nigrum ilarvirus 1 (SnIV1) genome assembly from selected publicly available global sequencing data

Associated literature[a]	Sequencing data accession number (year released)	Number of quality-screened reads (average read length)[b]	SnIV1 genome mapping[c]			GenBank accession number[d]
			Genome segment	Number of reads mapped (mean read depth or average coverage)[e]	Genome covered (%)	
(Howe et al. 2023)	SRR10849159 (2020)	156,095,145 (148 nt)	RNA 1	4,323 (188×)	99.7	BK061616
			RNA 2	2,986 (157×)	99.9	BK061617
			RNA 3	3,639 (240×)	99.8	BK061618[(23)]
	SRR10376303 (2020)	119,872,896 (147 nt)	RNA 1	3,154 (136×)	99.8	BK061619
			RNA 2	2,071 (108×)	99.9	BK061620
			RNA 3	4,709 (308×)	99.9	BK061621[(30)]
	SRR10849156 (2017)	188,311,868 (149 nt)	RNA 1	12,127 (527×)	99.9	BK061622
			RNA 2	7,173 (378×)	100.0	BK061623
			RNA 3	10,526 (694×)	100.0	BK061624[(31)]
(Mahlanza et al. 2022)	SRR15040766 (2021)	40,658,793 (150 nt)	RNA 1	648 (28×)	98.9	BK061666
			RNA 2	360 (19×)	98.3	BK061667
			RNA 3	480 (31×)	100.0	BK061668[(17)]
(Tauber et al. 2022)	SRR12659856 (2020)	72,394,575 (149 nt)	RNA 1	185 (8×)	98.8	BK061649
			RNA 2	297 (16×)	97.6	BK061650
			RNA 3	341 (23×)	99.6	BK061651[(32)]
(Sproviero et al. 2021)	SRR12387953 (2020)	57,174,266 (76 nt)	RNA 1	3,650 (80×)	99.7	BK061652
			RNA 2	3,015 (80×)	99.8	BK061653
			RNA 3	2,301 (77×)	99.6	BK061654[(27)]
(Auber et al. 2020)	SRR10758312 (2020)	32,532,748 (149 nt)	RNA 1	174,712 (7,584×)	100.0	BK061625
			RNA 2	223,487 (11,767×)	100.0	BK061626
			RNA 3	1,173,869 (77,350×)	100.0	BK061627[(33)]
	SRR10758313 (2020)	17,066,352 (150 nt)	RNA 1	174,375 (7,570×)	100.0	BK061628
			RNA 2	221,302 (11,653×)	100.0	BK061629
			RNA 3	1,169,597 (77,074×)	100.0	BK061630[(34)]
(Coady et al. 2020)	SRR11680723 (2020)	23,780,022 (141 nt)	RNA 1	5,711 (201×)	99.7	BK061655
			RNA 2	4,318 (188×)	99.5	BK061656
			RNA 3	2,459 (132×)	99.6	BK061657[(24)]
(Costa et al. 2020)	SRR11881307 (2020)	65,632,030 (98 nt)	RNA 1	167 (5×)	93.8	(–)
			RNA 2	98 (3×)	87.5	(–)
			RNA 3	122 (5×)	92.5	BK061658
(Chiapello et al. 2020)	SRR9995129[f] (2019)	44,182,895 (101 nt)	RNA 1	1,528 (43×)	98.8	BK061610
			RNA 2	1,220 (42×)	98.2	BK061611
			RNA 3	1,410 (60×)	98.9	BK061612[(21)]
	SRR11364885[f] (2020)	139,040,256 (98 nt)	RNA 1	3,100 (91×)	99.7	BK061613
			RNA 2	2,451 (87×)	99.6	BK061614
			RNA 3	2,542 (126×)	99.5	BK061615[(20)]
(Deboutte et al. 2020)	SRR10418310 (2019)	11,239,438 (113 nt)	RNA 1	4,327 (153×)	99.8	BK061659
			RNA 2	4,346 (189×)	97.1	BK061660
			RNA 3	12,796 (675×)	99.6	BK061661[(1)]
(Arnoux 2019)	ERR2576961 (2018)	29,364,317 (97 nt)	RNA 1	3,947 (112×)	98.9	BK061631
			RNA 2	1,672 (57×)	98.4	BK061632
			RNA 3	8,478 (361×)	100.0	BK061633[(18)]
(Wu et al. 2018)	SRR5380917 (2017)	12,751,998 (99 nt)	RNA 1	15,372 (441×)	100.0	BK061634
			RNA 2	6,581 (229×)	99.7	BK061635
			RNA 3	13,301 (577×)	99.8	BK061636[(28)]
	SRR5380918 (2017)	11,644,036 (98 nt)	RNA 1	593 (18×)	99.3	BK061637
			RNA 2	264 (9×)	99.5	BK061638
			RNA 3	641 (28×)	99.3	BK061639[(29)]
(Rai et al. 2018)	SRR6799516 (2018)	7,540,310 (99 nt)	RNA 1	206 (6×)	98.1	BK061640
			RNA 2	351 (12×)	98.2	BK061641
			RNA 3	3,178 (138×)	99.6	BK061642[(19)]
(Ledón-Rettig et al. 2017)	SRR4412518 (2016)	3,851,029 (75 nt)	RNA 1	476 (10×)	97.8	(–)
			RNA 2	298 (8×)	96.8	(–)
			RNA 3	205 (7×)	94.3	BK061662
(Chen et al. 2016)	SRR6387685 (2017)	39,742,426 (125 nt)	RNA 1	1,255 (46×)	99.9	BK061643
			RNA 2	1,569 (69×)	99.9	BK061644
			RNA 3	2,850 (157×)	99.8	BK061645[(14)]
(Vannette et al. 2015)	SRR1239309 (2014)	44,453,630 (96 nt)	RNA 1	227 (6×)	99.9	BK061663
			RNA 2	254 (9×)	99.7	BK061664
			RNA 3	105 (4×)	97.3	BK061665
(Roux et al. 2014)	SRR949232 (2013)	99,084,402 (47 nt)	RNA 1	5,038 (73×)	99.9	BK061646
			RNA 2	6,330 (111×)	99.7	BK061647
			RNA 3	2,060 (45×)	98.7	BK061648[(9)]

[a] Details of the sequencing metadata from each study can be found in Supplementary Table S2.
[b] Number of reads after quality screening and trimming of barcodes. The number in parentheses represents the average read length in number of nucleotides.
[c] One of the SnIV1 genomes from GenBank (a.n. OL472060 to OL472062) was used in reference-based genome assembly in CLC-GWB, with at least 90% identity and coverage threshold for reads mapping.
[d] Accession numbers deposited in GenBank as third-party annotations (TPAs) with superscript numbers in parentheses corresponding to each SnIV1 RNA 3 genome segment that was used in the phylogenetic analyses, with the resulting tree shown in Figure 1 and Supplementary Figure S2. (–) indicates sequence was not deposited because partial or fragmented genome was assembled, or the typical open reading frames were not found or were problematic.
[e] On average, number of times each locus in a reference genome is covered by the mapped reads.
[f] Genomes assembled from the two SRA datasets (SRR9995129, SRR11364885) and another dataset (SRR9995131) that was used to assemble SnIV1 isolate DMG 25 (MN520742 to MN520744, deposited with the name "grapevine associated ilarvirus") came from the same study (Chiapello et al. 2020). However, these genomes are not 100% identical in all segments (Supplementary Fig. S1) and, thus, can be considered three different isolates.

talis, and *S. nigrum*) developed symptoms in their newly formed, uninoculated leaves and tested positive for SnIV1 at 28 and 35 dpi. The rest of the mechanically inoculated plant species tested negative up to 35 dpi. Symptomatic *N. benthamiana* and *N. occidentalis* plants showed general stunting and smaller, crinkled, and chlorotic leaves compared with mock-inoculated plants (Fig. 3A and B), whereas symptomatic *S. nigrum* plants showed only subtle interveinal chlorosis in their newly formed uninoculated leaves (Fig. 3E), which tested positive for SnIV1 at around 18 and 28 dpi. *N. benthamiana* plants infected with SnIV1 later developed more deformed leaves with interveinal yellowing (Fig. 3C).

SnIV1-infected *N. benthamiana*, and *N. occidentalis* were later determined to be co-infected with TBRV2 by nanopore sequencing. Full genome sequences of TBRV2 were recovered from the inoculum source (*S. villosum*) and inoculated *N. benthamiana* plants. These two near-identical sequences are 90 to 95% identical to TBRV2 genomes deposited in GenBank from a previous study (Rivarez et al. 2023). This is the first detection of TBRV2 in a wild *S. villosum* plant and in France. However, TBRV2 was not identified from the HTS datasets of the other sequenced samples discussed above.

A single infection of SnIV1 in a *N. Benthamiana* plant was observed in a separate mechanical inoculation experiment, where the plants showed distinct bending of stems at around 28 dpi and severely crumpled leaves persisting until around 105 dpi (Fig. 3D).

Possible transmission of SnIV1 from infected seeds to newly germinated young plants was demonstrated. Seedlings of both *S. villosum* and *S. nigrum*, tested in pools of 10 leaves from different plants, tested positive for SnIV1 at 34 days after sowing.

Histopathology of SnIV1-infected *N. benthamiana* and SnIV1 virion morphology

Tissues of singly infected *N. benthamiana* collected at 49 dpi (plant shown in Figure 3D at 105 dpi) were examined in comparison with those of mock-inoculated plants of the same age grown

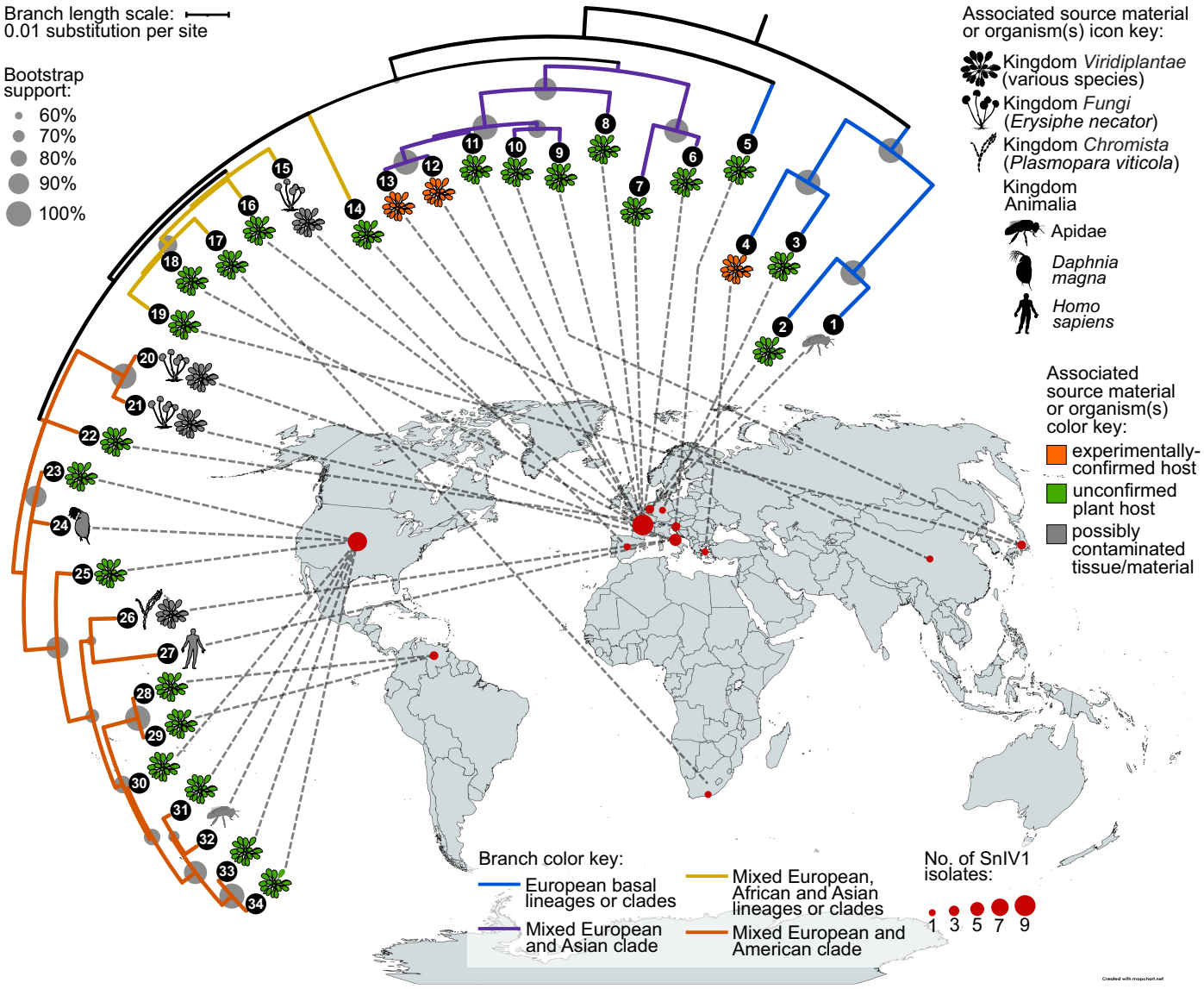

Fig. 1. Phylogenetic clustering, source materials or organism(s), and geographical origins of 34 Solanum nigrum ilarvirus 1 (SnIV1) global isolates. The midpoint rooted maximum likelihood phylogenetic tree was constructed based on a multiple sequence alignment of concatenated full coding nucleotide sequences of the movement and coat proteins (RNA 3 segment). The substitution model used was Tamura 3-parameter with discrete Gamma distribution with five rating categories and by assuming that a certain fraction of sites is evolutionarily invariable. The tree topology shown was inferred after 1,000 bootstrap replicates. Tree nodes/tips are numbered to refer to the accession numbers of SnIV1 genome sequences indicated in Supplementary Figure S1C, with their GenBank accession numbers and metadata in Supplementary Table S2 (indicated as the same superscript numbers). The world map was created using MapChart (https://www.mapchart.net/) and icons were downloaded from PhyloPic (https://www.phylopic.org/).

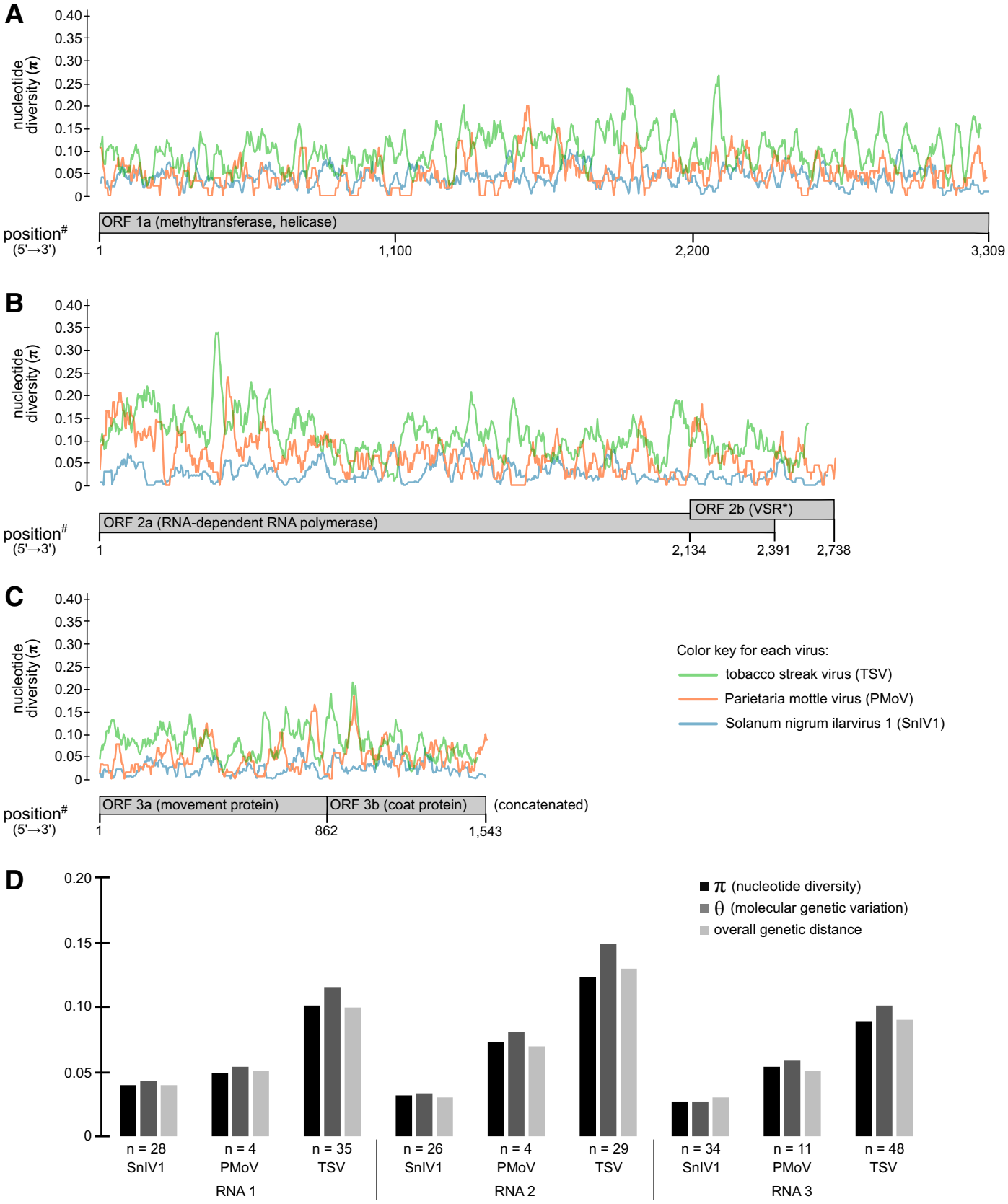

Fig. 2. Comparative diversity analyses of global isolates of Solanum nigrum ilarvirus 1 (SnIV1) with those of two closely related ilarviruses, tobacco streak virus (TSV), with a known wide range of associated hosts, and Parietaria mottle virus (PMoV), with a known narrow range of associated hosts. Nucleotide diversity (π) calculated in a window size of 30 and step of 3 nucleotides along **A,** RNA 1; **B,** RNA 2; and **C,** RNA 3 genome segments of TSV, PMoV, and SnIV1. **D,** Measures of overall π, molecular genetic variation (θ), and overall genetic distance in all genome segments of TSV, PMoV, and SnIV1. Note: #position in the SnIV1 alignment. *viral suppressor of RNA silencing protein.

under the same conditions. In healthy tissues, normal epidermal and parenchymal cells and vascular tissues were observed (Fig. 4A to C), whereas SnIV1-infected tissues and cells were strikingly distorted (Fig. 4D to F). Whereas no viral particles could be observed when ultra-thin sections were examined by TEM, a high number of viral particles were readily observed on leaf dip grids with negative staining prepared using extracts from the same *N. benthamiana* leaf (Fig. 4G and H). The virions observed were spherical, and measurements performed on 70 virions yielded an average diameter of 27.6 nm, with a standard deviation of 0.6 nm. Such morphological properties are consistent with those of some ilarviruses, although for some members of the genus, unstable particles or particles of slightly different sizes or with a bacilliform shape were also reported (Adams and Antoniw 2006; Simkovich et al. 2021).

Discussion

Collectively, we generated novel information on the global distribution of SnIV1, its genomic diversity compared with other ilarviruses, and phylogenetic relationships among SnIV1 isolates. We also generated new information on the biology and epidemiology of SnIV1, including its infectivity in various solanaceous plants and possible transmission through seeds and pollen. These results contribute to a better understanding of SnIV1's possible propensity to emerge as a global crop pathogen.

Expansion of possible hosts and geographic distribution of SnIV1

The HTS-based virome surveys implemented in this study uncovered association of SnIV1 with a new set of plant species from

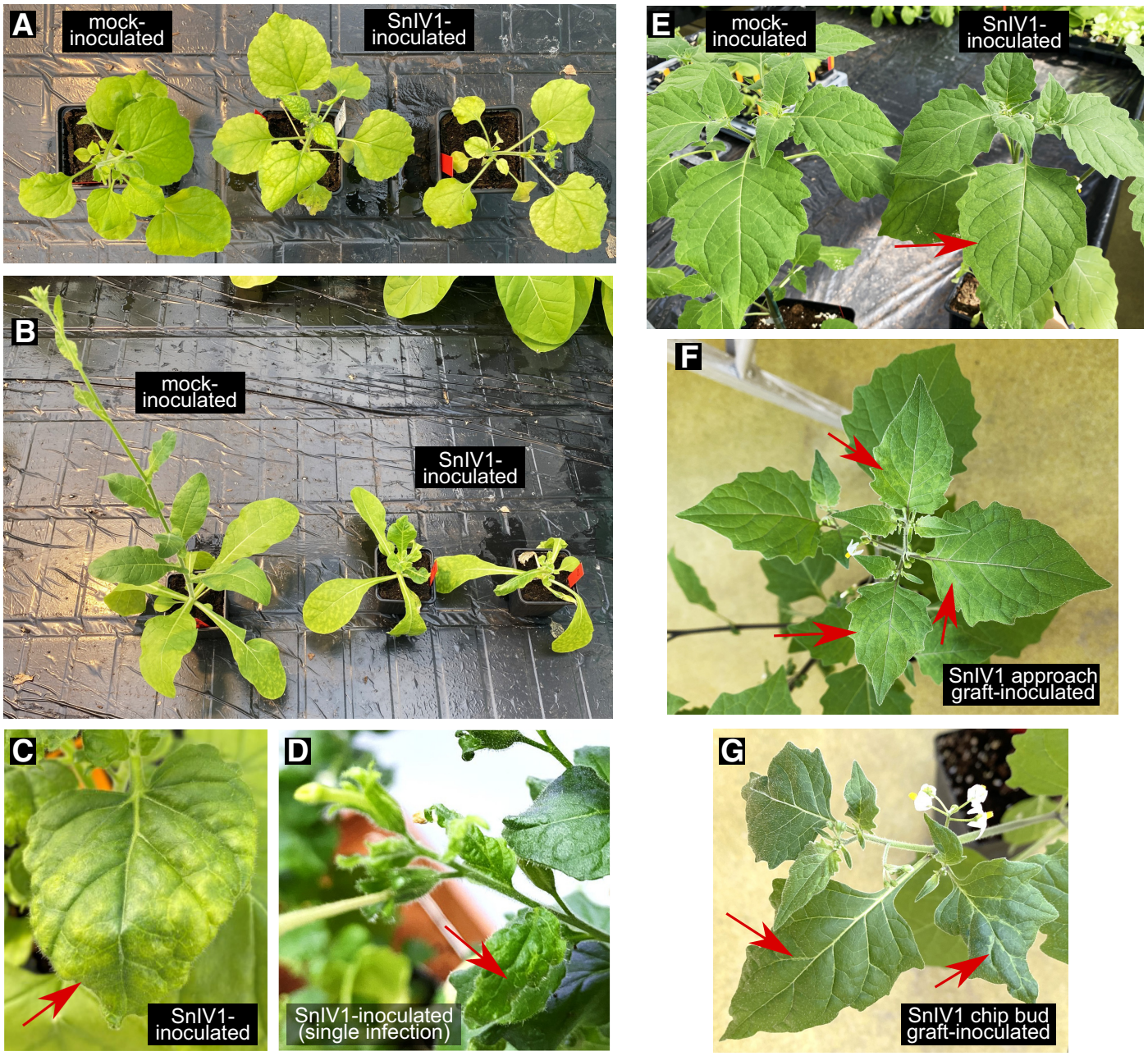

Fig. 3. Symptoms observed in inoculated plants. **A,** Mock- and mechanically inoculated *Nicotiana benthamiana* plants at 28 days postinoculation (dpi). **B,** Mock- and mechanically inoculated *N. occidentalis* plants at 28 dpi. **C,** Mechanically inoculated symptomatic *N. benthamiana* at 47 dpi. **D,** Mechanically inoculated symptomatic *N. benthamiana* at 105 dpi that was confirmed to be singly infected by Solanum nigrum ilarvirus 1 (SnIV1). **E,** Mock- and mechanically inoculated *Solanum nigrum* plants at 35 dpi. **F,** Graft-inoculated *S. nigrum* plants at 35 dpi. **G,** Chip bud graft-inoculated *S. nigrum* plants at 35 dpi. Red arrows indicate distinct symptomatic parts of each plant shown. Inoculated plants shown in A and B tested positive for TBRV2, but the rest of the plants shown did not undergo a similar test for TBRV2.

France and Belgium. Virome surveys conducted in Belgium detected SnIV1 in *S. melongena* and *S. tuberosum*, which are first detections of the virus in such species and in Belgium. This further expanded the number of *Solanaceae* species that are possible but still experimentally unverified hosts of SnIV1, a list that includes both cultivated (i.e., *S. lycopersicum*) and wild species (i.e., *S. chenopodioides*, *Physalis* sp.). The expanded association of solanaceous plants with SnIV1 fits very well with the results of the transmission experiments in this study, where infectivity of SnIV1 was confirmed in several solanaceous plants.

The in silico and literature searches implemented here likewise contribute additional information on diverse source materials and possible hosts of SnIV1, especially those that were sampled in countries outside of Europe. Most of the plant-derived sequencing datasets with SnIV1 sequences were obtained from metagenomic or metatranscriptomic sequencing of leaf tissues of plants from different families. Interestingly, SnIV1 was detected in the metatranscriptomic sequencing of belowground parts of *Fabaceae* species (*Medicago truncatula* and *Arachis hypogaea*) (Chen et al. 2016; Roux et al. 2014) and in *Lithospermum erythrorhizon* roots (Auber et al. 2020). The HTS of *L. erythrorhizon* has the highest number of SnIV1 reads among all the datasets. In the present study, systemic infection of SnIV1 was likewise demonstrated using RT-PCR assays in different below- and aboveground parts of *S. villosum,* including roots, whole flowers, individual floral parts, and pollen. SnIV1 sequences were likewise found in a metatranscriptomic sequencing study of *Petunia* × *hybrida* (*Solanaceae*) flowers (Haselmair-Gosch et al. 2018). Collectively, such diverse source organisms or materials give an unusual impression of a member of the *Ilarvirus* genus because its members are typically associated with a narrow range of natural hosts within one or a few families (Badillo-Vargas et al. 2016; Bratsch et al. 2019).

Moreover, SnIV1 was detected in the metatranscriptomic sequencing of insect samples from the United States and Belgium and, interestingly, in whole honeybees (*Apis mellifera*) (Deboutte et al. 2020), honeybee intestines (Tauber et al. 2022) and midgut (Vannette et al. 2015), and in the abdomen of bumblebees (*Bombus impatiens*) (Costa et al. 2020). This information could imply the possibility of *Apidae* species harboring SnIV1 after alighting and feeding on SnIV1-infected plants or collecting SnIV1-infected pollen from them. Such a scenario has been reported for ilarviruses associated with bee species (*Apidae*) and thrips (mostly *Thripidae*) in several studies (Bristow and Martin 1999; Roberts et al. 2018; Sdoodee and Teakle 1993; Sharman et al. 2015). Furthermore, the detection of SnIV1 sequences in bees might suggest localization of SnIV1, not only in bee integumentary parts, but also in internal parts such as the gut; however, this needs further experimental verification. The detections of SnIV1 sequences in other sequenced animal tissues, such as in *Daphnia magna* and human blood, are suspicious and remain to be resolved, but it is very possible that these represent contaminations that occurred in the viromic experiments.

It is important to note that these findings from the viromic surveys and in silico search of SRA datasets do not necessarily imply that the sequenced materials are true hosts of SnlV1. Although mining of SRA datasets for viruses provided useful insights, verification of such sequence mining-derived information using another diagnostic method is mandatory but difficult (Lebas et al. 2022). Aside from true virus infection or symbiotic association with a certain organism, detection of a viral sequence in an HTS dataset might result from wet lab contamination, index or barcode hopping, and cross-talk during sequencing (Lebas et al. 2022). It is likewise possible that other organisms that are the true hosts of SnIV1 could be present through an intimate (e.g., pathogen or symbiont) or casual association (e.g., as a surface contaminant) with the primary sequenced sample. In such a case, validation of HTS detection using a second diagnostic method and infectivity tests (if possible) are recommended (Fox 2020; Kutnjak et al. 2021).

TABLE 4. RT-PCR detection of Solanum nigrum ilarvirus 1 (SnIV1) and tomato betanucleorhabdovirus 2 (TBRV2) in plant samples from the mechanical, seed, and graft transmission experiments

Mode of transmission[a]	Plant species and cultivar (if known)	Symptoms observed in newly formed leaves	Individual or pooled samples[b]	dpi or das[c]	Number of SnIV1(+)/number of samples tested	Number of TBRV2(+)/number of samples tested[d]
Mechanical	*Chenopodium quinoa*	Asymptomatic	Pooled (4)	20	0/4	0/4
	Capsicum annuum	Asymptomatic	Pooled[e] (5)	14	0/2	(–)
		Asymptomatic	Individual[f]	20	0/15	0/1[#]
	Nicotiana benthamiana	Chlorosis, crinkling, and general stunting	Individual[e]	28	22/22	21/22
			Pooled[f] (5)	18	4/4	(–)
			Individual[g]	35	1[h]/2	1[i]/2
	N. glutinosa	Asymptomatic	Pooled (5)	14	0/2	(–)
	N. occidentalis	Vein yellowing, necrotic spots, and general stunting	Individual[e]	28	10/10	(–)
			Pooled[f] (5)	18	4/4	4/4
	N. tabacum 'Xanthi'	Asymptomatic	Pooled (5)	14	0/2	(–)
	Solanum lycopersicum 'M82'	Asymptomatic	Pooled (4)	20	0/4	0/4
	S. lycopersicum 'Rudgers'	Asymptomatic	Pooled (4)	20	0/4	0/4
	S. nigrum	Vein yellowing, slight crinkling	Individual[e]	28	1/1	(–)
			Pooled[f] (5)	18	4/4	4/4
Seed	*S. villosum*	Asymptomatic	Pooled (10)	34	5/5	(–)
	S. nigrum	Asymptomatic	Pooled (10)	34	7/7	(–)
Graft	*S. nigrum* (approach grafted)	Vein yellowing, slight crinkling	Individual	27	2/2	(–)
	S. nigrum (chip bud grafted)	Vein yellowing, slight crinkling	Individual	27	3/3	(–)

[a] Newly formed or uninoculated young leaves were tested in these experiments.
[b] Numbers enclosed in parentheses () indicate the number of plants that were pooled, prior to RNA extraction, to constitute the composite/pooled samples that were tested in RT-PCR.
[c] The number indicates the last time point at which RT-PCR testing was done in days postinoculation (dpi) for inoculated plants or days after sowing (das) for seed transmission experiment.
[d] (–) indicates not tested. [#] indicates test for TBRV2 was done in a pool of all the 15 samples collected.
[e] First experiment.
[f] Second experiment.
[g] Third experiment.
[h] This plant is TBRV2 negative, thus representing a single infection of SnIV1.
[i] This plant is SnIV1 negative, thus representing a single infection of TBRV2.

On the possibility of pollen as a vehicle for SnIV1 spread

Several ilarviruses and other members of the family *Bromoviridae* were shown to be horizontally transmitted through pollen (Aparicio et al. 1999; Card et al. 2007; George and Davidson 1963; Gilmer and Way 1960; Greber et al. 1991; Jaspers et al. 2015; Kawamura et al. 2014; Mink 1993; Sdoodee and Teakle 1988, 1993). In some cases, ilarviruses were also reported to be associated with pollen surface or exine (Digiaro and Savino 1992; Fetters et al. 2022; Hamilton 1977). Pollen transmission, whether actively or passively with the aid of arthropod vectors (Mink 1993), and the pollen's inherent ubiquitous presence in the environment could result in erroneous assignation of the natural host range of a virus, especially if sensitive diagnostic assays such as HTS or PCR are used. However, it is still an important horizontal transmission route that warrants special attention for emerging plant viruses. For instance, PMoV, the closest phylogenetically related virus to SnIV1, was shown to be pollen-transmitted and thus poses a threat to tomato production, at least in some European countries (Aparicio et al. 2018; Aramburu et al. 2010; Parrella et al. 2020).

Based on the results of this study, it is thus hypothesized that contamination by SnIV1-infected pollen might be one of the reasons (if not the most probable) for the identification of SnIV1 in different sequencing datasets. Detection of SnIV1 sequences in 39 datasets of leaf surface or epiphyte RNA sequencing from two *Poaceae* species (*Panicum* and *Miscanthus*) (Howe et al. 2023) fits well with such a hypothesis of surface contamination by pollen containing SnIV1. Thus, it is postulated that infected nearby crops or non-crop plants (most probably a *Solanaceae* species) could be a source of SnIV1-infected pollen that could make its way, passively or assisted by arthropod vectors, to neighboring plants. However, this hypothesis will need to be further investigated before it can be fully accepted.

Aside from plant species of the *Fabaceae*, *Rosaceae*, and *Cannabaceae*, SnIV1 was also associated with grapevines (infected with *Erysiphe necator* and *Plasmopara viticola*) in two viromic

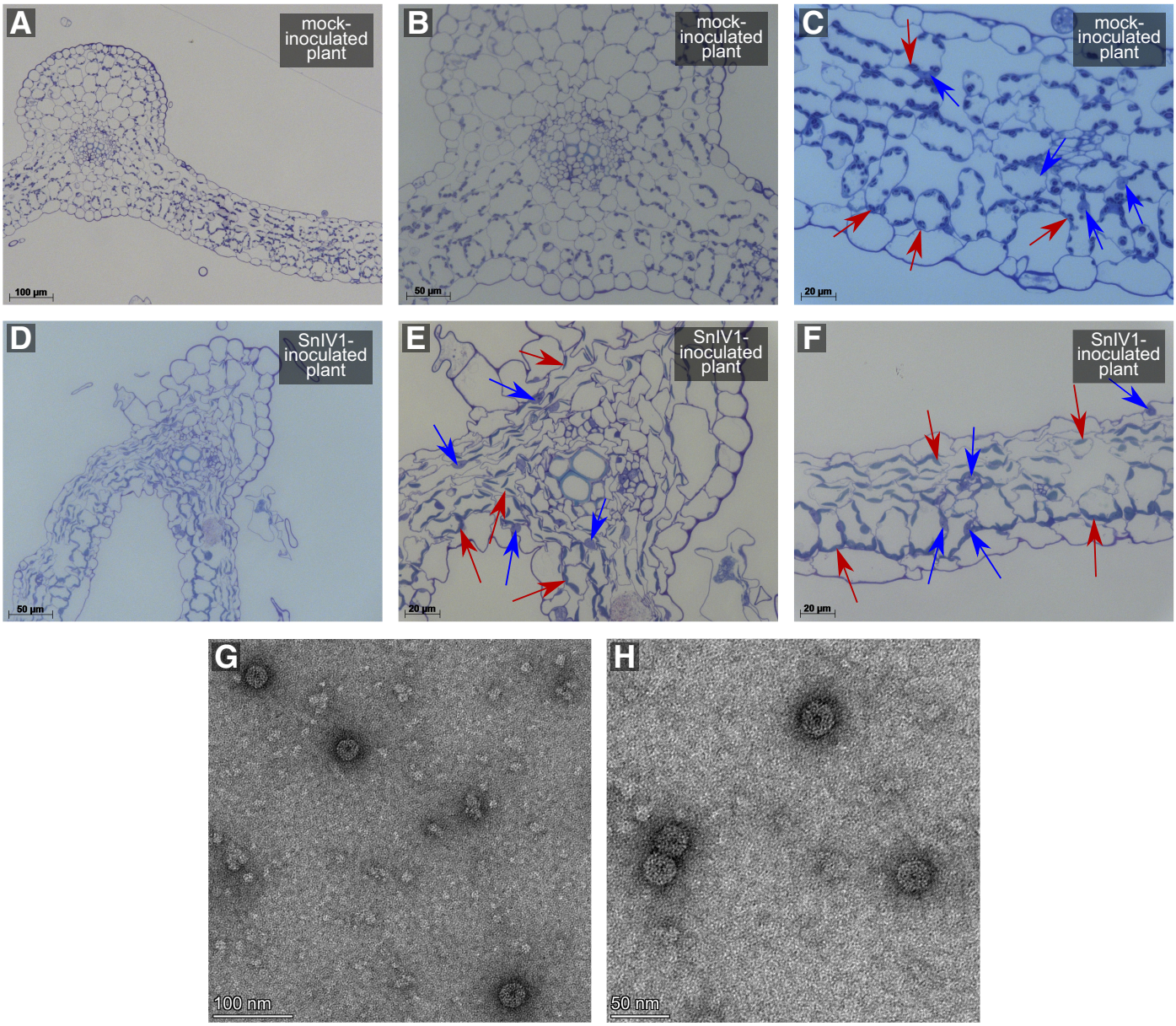

Fig. 4. Solanum nigrum ilarvirus 1 (SnIV1)-infected tissues and virions from mechanically inoculated *Nicotiana benthamiana* leaves. **A to C,** Thin sections of mock-inoculated *N. benthamiana* leaves for comparison that were taken at different magnifications under a light microscope. **D to F,** Thin sections of SnIV1-inoculated *N. benthamiana* leaves that were taken at different magnifications under a light microscope. Arrows indicate the nuclei (blue arrows) and chloroplasts (red arrows). **G and H,** Transmission electron micrograph of SnIV1 spherical virions from a crude preparation of mechanically inoculated *N. benthamiana* tissues, shown at 100 and 50 nm scales.

studies (Chiapello et al. 2019, 2020) and in an additional two grapevine cultivars (Ugni Blanc and Sauvignon) from France that were sequenced in this study. However, cuttings from two French grapevines that had positive HTS and RT-PCR detections did not show evidence of SnlV1 presence when tested using RT-PCR several months after replanting as cuttings. This suggests either a localized or non-persistent infection in grapevine or, once again, that the first detection in field samples corresponds to surface contamination. Interestingly, another probable case of contamination is the detection of SnlV1 in *D. carota* subsp. *carota* (wild carrot). Out of 45 wild carrot populations (composite samples) (Schönegger 2023), only one showed SnlV1 reads, and this population happens to have been sampled close to the Sauvignon grapevines and SnlV1-infected *S. villosum* and *S. nigrum* plants at the INRAE Bordeaux research center.

Ilarvirus virions are known to be labile, but ilarviruses are also known to be pollen transmitted. This suggests that SnIV1 could potentially be efficiently protected and dispersed by pollen across distances and in various surface and source materials (Simkovich et al. 2021).

Patterns of variability and clustering of SnlV1 global isolates

Relatively low diversity was observed among isolates of SnIV1, across all genome segments, when compared with closely related ilarviruses, such as TSV, for which a comparable number of sequences was available. This result needs to be interpreted carefully due to the possible uneven sampling (by both number and location) of the three compared viruses. Moreover, phylogenetic analyses showed only a partial clustering of SnIV1 isolates based on geographic origin, with low ancestral location probability when tested using a Bayesian framework. Although there is a distinct basal clade of isolates from European countries, no distinct pattern could be observed when the time of sampling (or sequencing) or broad category of possible hosts or source organism(s) (i.e., plants or animals) was considered.

Host range and other modes of transmission of SnlV1

Two *Solanaceae* species were recently shown to be hosts of SnIV1, *C. annuum* (hybrid Arlequin F1) and *N. benthamiana* (Orfanidou et al. 2022). However, SnIV1 was not successfully mechanically transmitted to pepper plants in this study. This result might be explained by differences in inoculation procedures, inoculum source, or pepper genotypes used in the two studies. Furthermore, among eight plant species that were mechanically inoculated in the present study, infectivity of SnIV1 was demonstrated in three solanaceous species only: *N. occidentalis*, *S. nigrum*, and *N. benthamiana*. In a previous study (Ma et al. 2020), SnIV1 sequences were detected in both tomato and *S. nigrum* plants. However, in the present study, SnIV1 was successfully transmitted to *S. nigrum* but not to the two tomato varieties (cultivars Rudgers and M82). This suggests that association of SnIV1 with tomato in the Ma et al. (2020) study might be a result of surface contamination or, alternatively, differences in plant or virus genotype. Nevertheless, the infectivity of SnIV1 in a genotype of pepper raises the possibility that SnIV1 could be adapting to cultivated solanaceous hosts. It is worthwhile to note that both *S. villosum* and *S. nigrum* overwinter in at least some parts of Europe and may serve as reservoir of the virus during the winter months. Overwintering of SnIV1 is likely also possible through infected seeds because vertical transmission through seeds of these two wild species was demonstrated here.

Summary and future perspectives

Overall, the viromic surveys, extensive sequence database exploration, and literature searches conducted in this study resulted in the expansion of knowledge on the geographic distribution, possible hosts or source organisms, and diversity of SnlV1. In parallel, classical plant virology techniques facilitated the characterization of its pathobiology and possible modes of transmission. The properties of SnIV1 appear to be similar to those of other ilarviruses, but it is interestingly (and quite unexpectedly) associated much more frequently with very diverse plant samples and even with animal species, mostly from *Apidae*. This raises further questions on unexplored properties of SnIV1 leading to its propensity to come up in unexpected HTS datasets. As discussed, many other ilarviruses are pollen-borne, including some infecting solanaceous species, although none has been reported in association with grapevines, despite the heavy HTS sequencing efforts performed in many laboratories around the world on this species. Although the present work facilitated progress in understanding aspects of the biology and epidemiology of SnIV1, there is still more information to be uncovered to fully understand this intriguing virus. Similar work could be implemented on other plant viruses poorly characterized but of similar biology and epidemiology to gain a certain level of preparedness for the possible global spread and disease outbreaks they may cause in the future.

Data and analyses pipeline availability

The raw sequencing reads generated from this study were submitted to the NCBI Sequence Read Archive (SRA) collectively under the BioProject accession number PRJNA874692 and to the Recherche Data Gouv platform (https://entrepot.recherche.data.gouv.fr/dataverse/inrae) with the persistent digital object identifier (doi) https://doi.org/10.57745/ZIXT4A. All SnIV1 genome sequences generated from this study were submitted to NCBI GenBank, under the accession numbers listed in Tables 1 and 3 and Supplementary Table S2. Details of the bioinformatic pipeline used for virus genome assembly are available through this link: https://gitlab.com/ilvo/phbn-wp2-training/-/tree/master/CLC_NIB_1.

Acknowledgments

We thank the Sequencing Platform of Toulouse (GeT-PlaGe) for Illumina sequencing and Marie Lefebvre for assisting in the processing of sequencing data. The authors are grateful for the assistance provided by Thierry Mauduit, Christophe Higelin, and Maryam Khalili in the field, greenhouse, and sample preparation work; Laure Beven for assisting in the use of the dark field microscope and Mickael Maucourt for assisting with tissue lyophilization; and Varvara Maglioka and Reza M. Hajimorad for providing their SnIV1 genomic sequences ahead of release in GenBank and the publication of their papers.

Literature Cited

Adams, M. J., and Antoniw, J. F. 2006. DPVweb: A comprehensive database of plant and fungal virus genes and genomes. Nucleic Acids Res. 34: D382-D385.

Adkins, S., Baker, C. A., Badillo-Vargas, I. E., Frantz, G., Mellinger, H. C., Roe, N., and Funderburk, J. E. 2015. Necrotic streak disease of tomato in Florida caused by a new ilarvirus species related to Tulare apple mosaic virus. New Dis. Rep. 31:16.

Aparicio, F., Aramburu, J., Herranz, M. C., Pallás, V., and López, C. 2018. Parietaria mottle virus: A potential threat for tomato crops? Acta Hortic. 1207:261-268.

Aparicio, F., Sánchez-Pina, M. A., Sánchez-Navarro, J. A., and Pallás, V. 1999. Location of prunus necrotic ringspot ilarvirus within pollen grains of infected nectarine trees: Evidence from RT-PCR, dot-blot and in situ hybridisation. Eur. J. Plant Pathol. 105:623-627.

Aramburu, J., Galipienso, L., Aparicio, F., Soler, S., and López, C. 2010. Mode of transmission of parietaria mottle virus. J. Plant Pathol. 92:679-684.

Arnoux, S. 2019. Comparative analyses of the molecular footprint of domestication in three *Solanaceae* species: Eggplant, pepper and tomato. Ph.D. Thesis. https://tel.archives-ouvertes.fr/tel-02185095v2/document

Auber, R. P., Suttiyut, T., McCoy, R. M., Ghaste, M., Crook, J. W., Pendleton, A. L., Widhalm, J. R., and Wisecaver, J. H. 2020. Hybrid de novo genome assembly of red gromwell (*Lithospermum erythrorhizon*) reveals evolutionary insight into shikonin biosynthesis. Hortic. Res. 7:82.

Badillo-Vargas, I. E., Baker, C. A., Turechek, W. W., Frantz, G., Mellinger, H. C., Funderburk, J. E., and Adkins, S. 2016. Genomic and biological characterization of tomato necrotic streak virus, a novel subgroup 2 ilarvirus infecting tomato in Florida. Plant Dis. 100:1046-1053.

Bester, R., and Maree, H. J. 2023. First report of the plum marbling disease associated agent, plum viroid I, in apricots (*Prunus armeniaca*) in South Africa. Plant Dis. 107:1956.

Bouckaert, R., Vaughan, T. G., Barido-Sottani, J., Duchêne, S., Fourment, M., Gavryushkina, A., Heled, J., Jones, G., Kühnert, D., De Maio, N., Matschiner, M., Mendes, F. K., Müller, N. F., Ogilvie, H. A., du Plessis, L., Popinga, A., Rambaut, A., Rasmussen, D., Siveroni, I., Suchard, M. A., Wu, C.-H., Xie, D., Zhang, C., Stadler, T., and Drummond, A. J. 2019. BEAST 2.5: An advanced software platform for Bayesian evolutionary analysis. PLoS Comput. Biol. 15:e1006650.

Bratsch, S. A., Creswell, T. C., and Ruhl, G. E. 2018. First report of tomato necrotic spot virus infecting tomato in Indiana. Plant Health Prog. 19:224-225.

Bratsch, S. A., Grinstead, S., Creswell, T. C., Ruhl, G. E., and Mollov, D. 2019. Characterization of tomato necrotic spot virus, a subgroup 1 ilarvirus causing necrotic foliar, stem, and fruit symptoms in tomatoes in the United States. Plant Dis. 103:1391-1396.

Bristow, P. R., and Martin, R. R. 1999. Transmission and the role of honeybees in field spread of blueberry shock ilarvirus, a pollen-borne virus of highbush blueberry. Phytopathology 89:124-130.

Buzkan, N., Chiumenti, M., Massart, S., Sarpkaya, K., Karadağ, S., and Minafra, A. 2019. A new emaravirus discovered in Pistacia from Turkey. Virus Res. 263:159-163.

Card, S. D., Pearson, M. N., and Clover, G. R. G. 2007. Plant pathogens transmitted by pollen. Australas. Plant Pathol. 36:455-461.

Carroll, D., Daszak, P., Wolfe, N. D., Gao, G. F., Morel, C. M., Morzaria, S., Pablos-Méndez, A., Tomori, O., and Mazet, J. A. K. 2018. The Global Virome Project. Science 359:872-874.

Chang, S., Puryear, J., and Cairney, J. 1993. A simple and efficient method for isolating RNA from pine trees. Plant Mol. Biol. Rep. 11:113-116.

Chen, X., Yang, Q., Li, H., Li, H., Hong, Y., Pan, L., Chen, N., Zhu, F., Chi, X., Zhu, W., Chen, M., Liu, H., Yang, Z., Zhang, E., Wang, T., Zhong, N., Wang, M., Liu, H., Wen, S., Li, X., Zhou, G., Li, S., Wu, H., Varshney, R., Liang, X., and Yu, S. 2016. Transcriptome-wide sequencing provides insights into geocarpy in peanut (*Arachis hypogaea* L.). Plant Biotechnol. J. 14:1215-1224.

Chiapello, M., Rodriguez-Romero, J., Ayllon, M., and Turina, M. 2019. A report on the virome of obligatory biotrophs. https://ec.europa.eu/research/participants/documents/downloadPublic?documentIds=080166e5c8e77dab&appId=PPGMS (accessed February 7, 2022).

Chiapello, M., Rodríguez-Romero, J., Nerva, L., Forgia, M., Chitarra, W., Ayllón, M. A., and Turina, M. 2020. Putative new plant viruses associated with *Plasmopara viticola*-infected grapevine samples. Ann. Appl. Biol. 176:180-191.

Coady, K. K., Burgoon, L., Doskey, C., and Davis, J. W. 2020. Assessment of transcriptomic and apical responses of *Daphnia magna* exposed to a polyethylene microplastic in a 21-d chronic study. Environ. Toxicol. Chem. 39:1578-1589.

Costa, C. P., Duennes, M. A., Fisher, K., Der, J. P., Watrous, K. M., Okamoto, N., Yamanaka, N., and Woodard, S. H. 2020. Transcriptome analysis reveals nutrition- and age-related patterns of gene expression in the fat body of pre-overwintering bumble bee queens. Mol. Ecol. 29:720-737.

Deboutte, W., Beller, L., Yinda, C. K., Maes, P., de Graaf, D. C., and Matthijnssens, J. 2020. Honey-bee–associated prokaryotic viral communities reveal wide viral diversity and a profound metabolic coding potential. Proc. Natl. Acad. Sci. 117:10511-10519.

de Klerk, A., Swanepoel, P., Lourens, R., Zondo, M., Abodunran, I., Lytras, S., MacLean, O. A., Robertson, D., Kosakovsky Pond, S. L., Zehr, J. D., Kumar, V., Stanhope, M. J., Harkins, G., Murrell, B., and Martin, D. P. 2022. Conserved recombination patterns across coronavirus subgenera. Virus Evol. 8:1-15.

Dias, N. P., Hu, R., Hensley, D. D., Hansen, Z. R., Domier, L. L., and Hajimorad, M. R. 2022. A survey for viruses and viroids of peach in Tennessee orchards by RNA sequencing. Plant Health Prog. 23:265-268.

Digiaro, M., and Savino, V. 1992. Role of pollen and seeds in the spread of ilarviruses in almond. Adv. Hortic. Sci. 6:134-136.

Edgar, R. C. 2004. MUSCLE: Multiple sequence alignment with high accuracy and high throughput. Nucleic Acids Res. 32:1792-1797.

Edgar, R. C., Taylor, J., Lin, V., Altman, T., Barbera, P., Meleshko, D., Lohr, D., Novakovsky, G., Buchfink, B., Al-Shayeb, B., Banfield, J. F., de la Peña, M., Korobeynikov, A., Chikhi, R., and Babaian, A. 2022. Petabase-scale sequence alignment catalyses viral discovery. Nature 602:142-147.

Fetters, A. M., Cantalupo, P. G., Wei, N., Robles, M. T. S., Stanley, A., Stephens, J. D., Pipas, J. M., and Ashman, T.-L. 2022. The pollen virome of wild plants and its association with variation in floral traits and land use. Nat. Commun. 13:523.

Foissac, X., Svanella-Dumas, L., Gentit, P., Dulucq, M.-J., Marais, A., and Candresse, T. 2005. Polyvalent degenerate oligonucleotides reverse transcription-polymerase chain reaction: A polyvalent detection and characterization tool for trichoviruses, capilloviruses, and foveaviruses. Phytopathology 95:617-625.

Fontdevila, N., Khalili, M., Maachi, A., Rivarez, M. P. S., Rollin, R., Salavert, F., Temple, C., Aranda, M. A., Boonham, N., Botermans, M., Candresse, T., Fox, A., Hernando, Y., Kutnjak, D., Marais, A., Petter, F., Ravnikar, M., Selmi, I., Tahzima, R., Trontin, C., Wetzel, T., and Massart, S. 2023. Managing the deluge of newly discovered plant viruses and viroids: An optimized scientific and regulatory framework for their characterization and risk analysis. Front. Microbiol. 14.

Fox, A. 2020. Reconsidering causal association in plant virology. Plant Pathol. 69:956-961.

Gaafar, Y. Z. A., Herz, K., Hartrick, J., Fletcher, J., Blouin, A. G., MacDiarmid, R., and Ziebell, H. 2020. Investigating the pea virome in Germany—Old friends and new players in the field(s). Front. Microbiol. 11:2605.

George, J. A., and Davidson, T. R. 1963. Pollen transmission of necrotic ring spot and sour cherry yellows viruses from tree to tree. Can. J. Plant Sci. 43:276-288.

Gilmer, R., and Way, R. 1960. Pollen transmission of necrotic ringspot and prune dwarf viruses in sour cherry. Phytopathology 50:624-625.

Greber, R. S., Klose, M. J., Milne, J. R., and Teakle, D. S. 1991. Transmission of prunus necrotic ringspot virus using plum pollen and thrips. Ann. Appl. Biol. 118:589-593.

Gregory, A. C., Zayed, A. A., Conceição-Neto, N., Temperton, B., Bolduc, B., Alberti, A., Ardyna, M., Arkhipova, K., Carmichael, M., Cruaud, C., Dimier, C., Domínguez-Huerta, G., Ferland, J., Kandels, S., Liu, Y., Marec, C., Pesant, S., Picheral, M., Pisarev, S., Poulain, J., Tremblay, J.-É., Vik, D., Babin, M., Bowler, C., Culley, A. I., de Vargas, C., Dutilh, B. E., Iudicone, D., Karp-Boss, L., Roux, S., Sunagawa, S., Wincker, P., Sullivan, M. B., Acinas, S. G., Babin, M., Bork, P., Boss, E., Bowler, C., Cochrane, G., de Vargas, C., Follows, M., Gorsky, G., Grimsley, N., Guidi, L., Hingamp, P., Iudicone, D., Jaillon, O., Kandels-Lewis, S., Karp-Boss, L., Karsenti, E., Not, F., Ogata, H., Pesant, S., Poulton, N., Raes, J., Sardet, C., Speich, S., Stemmann, L., Sullivan, M. B., Sunagawa, S., and Wincker, P. 2019. Marine DNA viral macro- and microdiversity from pole to pole. Cell 177:1109-1123.e14.

Hamilton, R. I. 1977. Surface contamination of pollen by plant viruses. Phytopathology 77:395.

Hammond, J., Adams, I. P., Fowkes, A. R., McGreig, S., Botermans, M., Oorspronk, J. J. A., Westenberg, M., Verbeek, M., Dullemans, A. M., Stijger, C. C. M. M., Blouin, A. G., Massart, S., De Jonghe, K., Heyneman, M., Walsh, J. A., and Fox, A. 2020. Sequence analysis of 43-year old samples of *Plantago lanceolata* show that Plantain virus X is synonymous with Actinidia virus X and is widely distributed. Plant Pathol. 70:249-258.

Haselmair-Gosch, C., Miosic, S., Nitarska, D., Roth, B. L., Walliser, B., Paltram, R., Lucaciu, R. C., Eidenberger, L., Rattei, T., Olbricht, K., Stich, K., and Halbwirth, H. 2018. Great cause—Small effect: Undeclared genetically engineered orange petunias harbor an inefficient dihydroflavonol 4-reductase. Front. Plant Sci. 9:149.

Hou, W., Li, S., and Massart, S. 2020. Is there a "biological desert" with the discovery of new plant viruses? A retrospective analysis for new fruit tree viruses. Front. Microbiol. 11:592816.

Hou, X., He, Y., Fang, P., Mei, S.-Q., Xu, Z., Wu, W.-C., Tian, J.-H., Zhang, S., Zeng, Z.-Y., Gou, Q.-Y., Xin, G.-Y., Le, S.-J., Xia, Y.-Y., Zhou, Y.-L., Hui, F.-M., Pan, Y.-F., Eden, J.-S., Yang, Z.-H., Han, C., Shu, Y.-L., Guo, D., Li, J., Holmes, E. C., Li, Z.-R., and Shi, M. 2023. Artificial intelligence redefines RNA virus discovery. bioRxiv 537342.

Howe, A., Stopnisek, N., Dooley, S. K., Yang, F., Grady, K. L., and Shade, A. 2023. Seasonal activities of the phyllosphere microbiome of perennial crops. Nat. Commun. 14:1039.

ICTV. 2023. Current ICTV Taxonomy Release. https://ictv.global/taxonomy (accessed April 10, 2023).

Jaspers, M. V., Falloon, P. G., and Pearson, M. N. 2015. Seed and pollen transmission of asparagus virus 2. Eur. J. Plant Pathol. 142:173-183.

Kawamura, R., Shimura, H., Mochizuki, T., Ohki, S. T., and Masuta, C. 2014. Pollen transmission of asparagus virus 2 (AV-2) may facilitate mixed infection by two AV-2 isolates in asparagus plants. Phytopathology 104:1001-1006.

Khalili, M., Candresse, T., Koloniuk, I., Safarova, D., Brans, Y., Faure, C., Delmas, M., Massart, S., Aranda, M. A., Caglayan, K., Decroocq, V., Drogoudi, P., Glasa, M., Pantelidis, G., Navratil, M., Latour, F., Spak, J., Pribylova, J., Mihalik, D., Palmisano, F., Saponari, A., Necas, T., Sedlak, J., and Marais, A. 2023. The expanding menagerie of Prunus-infecting luteoviruses. Phytopathology 113:345-354.

Kibbe, W. A. 2007. OligoCalc: An online oligonucleotide properties calculator. Nucleic Acids Res. 35:W43-W46.

Kumar, S., Kumar, G. S., Maitra, S. S., Malý, P., Bharadwaj, S., Sharma, P., and Dwivedi, V. D. 2022. Viral informatics: Bioinformatics-based solution for managing viral infections. Brief. Bioinform. 23:1-36.

Kumar, S., Stecher, G., Li, M., Knyaz, C., and Tamura, K. 2018. MEGA X: Molecular Evolutionary Genetics Analysis across Computing Platforms. Mol. Biol. Evol. 35:1547-1549.

Kutnjak, D., Tamisier, L., Adams, I., Boonham, N., Candresse, T., Chiumenti, M., De Jonghe, K., Kreuze, J. F., Lefebvre, M., Silva, G., Malapi-Wight,

M., Margaria, P., Mavrič Pleško, I., McGreig, S., Miozzi, L., Remenant, B., Reynard, J.-S., Rollin, J., Rott, M., Schumpp, O., Massart, S., and Haegeman, A. 2021. A primer on the analysis of high-throughput sequencing data for detection of plant viruses. Microorganisms 9:841.

Lauber, C., and Seitz, S. 2022. Opportunities and challenges of data-driven virus discovery. Biomolecules 12:1073.

Lebas, B., Adams, I., Al Rwahnih, M., Baeyen, S., Bilodeau, G. J., Blouin, A. G., Boonham, N., Candresse, T., Chandelier, A., De Jonghe, K., Fox, A., Gaafar, Y. Z. A., Gentit, P., Haegeman, A., Ho, W., Hurtado-Gonzales, O., Jonkers, W., Kreuze, J., Kutjnak, D., Landa, B., Liu, M., Maclot, F., Malapi-Wight, M., Maree, H. J., Martoni, F., Mehle, N., Minafra, A., Mollov, D., Moreira, A., Nakhla, M., Petter, F., Piper, A. M., Ponchart, J., Rae, R., Remenant, B., Rivera, Y., Rodoni, B., Roenhorst, J. W., Rollin, J., Saldarelli, P., Santala, J., Souza-Richards, R., Spadaro, D., Studholme, D. J., Sultmanis, S., van der Vlugt, R., Tamisier, L., Trontin, C., Vazquez-Iglesias, I., Vicente, C. S. L., Vossenberg, B. T. L. H., Wetzel, T., Ziebell, H., and Massart, S. 2022. Facilitating the adoption of high-throughput sequencing technologies as a plant pest diagnostic test in laboratories: A step-by-step description. EPPO Bull. 52:394-418.

Ledón-Rettig, C. C., Zattara, E. E., and Moczek, A. P. 2017. Asymmetric interactions between doublesex and tissue- and sex-specific target genes mediate sexual dimorphism in beetles. Nat. Commun. 8:14593.

Lee, B. D., Neri, U., Roux, S., Wolf, Y. I., Camargo, A. P., Krupovic, M., Simmonds, P., Kyrpides, N., Gophna, U., Dolja, V. V., and Koonin, E. V. 2023. Mining metatranscriptomes reveals a vast world of viroid-like circular RNAs. Cell 186:646-661.e4.

Letunic, I., and Bork, P. 2021. Interactive Tree Of Life (iTOL) v5: An online tool for phylogenetic tree display and annotation. Nucleic Acids Res. 49: W293-W296.

Ma, Y., Marais, A., Lefebvre, M., Faure, C., and Candresse, T. 2020. Metagenomic analysis of virome cross-talk between cultivated *Solanum lycopersicum* and wild *Solanum nigrum*. Virology 540:38-44.

Ma, Y., Marais, A., Lefebvre, M., Theil, S., Svanella-Dumas, L., Faure, C., and Candresse, T. 2019. Phytovirome analysis of wild plant populations: Comparison of double-stranded RNA and virion-associated nucleic acid metagenomic approaches. J. Virol. 94:e01462-19.

Maclot, F., Candresse, T., Filloux, D., Malmstrom, C. M., Roumagnac, P., van der Vlugt, R., and Massart, S. 2020. Illuminating an ecological blackbox: Using high throughput sequencing to characterize the plant virome across scales. Front. Microbiol. 11:578064.

Mahlanza, T., Pierneef, R. E., Makwarela, L., Roberts, R., and van der Merwe, M. 2022. Metagenomic analysis for detection and discovery of plant viruses in wild *Solanum* spp. in South Africa. Plant Pathol. 71: 1633-1644.

Marais, A., Faure, C., Couture, C., Bergey, B., Gentit, P., and Candresse, T. 2014. Characterization by deep sequencing of divergent plum bark necrosis stem pitting-associated virus (PBNSPaV) isolates and development of a broad-spectrum PBNSPaV detection assay. Phytopathology 104: 660-666.

Martin, D. P., Varsani, A., Roumagnac, P., Botha, G., Maslamoney, S., Schwab, T., Kelz, Z., Kumar, V., and Murrell, B. 2021. RDP5: A computer program for analyzing recombination in, and removing signals of recombination from, nucleotide sequence datasets. Virus Evol. 7:veaa087.

Massart, S., Candresse, T., Gil, J., Lacomme, C., Predajna, L., Ravnikar, M., Reynard, J.-S., Rumbou, A., Saldarelli, P., Škorić, D., Vainio, E. J., Valkonen, J. P. T., Vanderschuren, H., Varveri, C., and Wetzel, T. 2017. A framework for the evaluation of biosecurity, commercial, regulatory, and scientific impacts of plant viruses and viroids identified by NGS technologies. Front Microbiol. 8:45.

McLeish, M. J., Fraile, A., and García-Arenal, F. 2021. Population genomics of plant viruses: The ecology and evolution of virus emergence. Phytopathology 111:32-39.

Meurens, F., Dunoyer, C., Fourichon, C., Gerdts, V., Haddad, N., Kortekaas, J., Lewandowska, M., Monchatre-Leroy, E., Summerfield, A., Wichgers Schreur, P. J., van der Poel, W. H. M., and Zhu, J. 2021. Animal board invited review: Risks of zoonotic disease emergence at the interface of wildlife and livestock systems. Animal 15:100241.

Mifsud, J. C. O., Gallagher, R. V., Holmes, E. C., and Geoghegan, J. L. 2022. Transcriptome mining expands knowledge of RNA viruses across the plant kingdom. J. Virol. 96:e00260-22.

Mink, G. I. 1993. Pollen and seed-transmitted viruses and viroids. Annu. Rev. Phytopathol. 31:375-402.

Morens, D. M., Daszak, P., Markel, H., and Taubenberger, J. K. 2020. Pandemic COVID-19 joins history's pandemic legion. mBio 11:e00812-20.

Muhire, B. M., Varsani, A., and Martin, D. P. 2014. SDT: A virus classification tool based on pairwise sequence alignment and identity calculation. PLoS One 9:e108277.

Natsume, S., Takagi, H., Shiraishi, A., Murata, J., Toyonaga, H., Patzak, J., Takagi, M., Yaegashi, H., Uemura, A., Mitsuoka, C., Yoshida, K., Krofta, K., Satake, H., Terauchi, R., and Ono, E. 2015. The draft genome of hop (*Humulus lupulus*), an essence for brewing. Plant Cell Physiol. 56:428-441.

Neri, U., Wolf, Y. I., Roux, S., Camargo, A. P., Lee, B., Kazlauskas, D., Chen, I. M., Ivanova, N., Zeigler Allen, L., Paez-Espino, D., Bryant, D. A., Bhaya, D., Krupovic, M., Dolja, V. V., Kyrpides, N. C., Koonin, E. V., Gophna, U., Narrowe, A. B., Probst, A. J., Sczyrba, A., Kohler, A., Séguin, A., Shade, A., Campbell, B. J., Lindahl, B. D., Reese, B. K., Roque, B. M., DeRito, C., Averill, C., Cullen, D., Beck, D. A. C., Walsh, D. A., Ward, D. M., Wu, D., Eloe-Fadrosh, E., Brodie, E. L., Young, E. B., Lilleskov, E. A., Castillo, F. J., Martin, F. M., LeCleir, G. R., Attwood, G. T., Cadillo-Quiroz, H., Simon, H. M., Hewson, I., Grigoriev, I. V., Tiedje, J. M., Jansson, J. K., Lee, J., VanderGheynst, J. S., Dangl, J., Bowman, J. S., Blanchard, J. L., Bowen, J. L., Xu, J., Banfield, J. F., Deming, J. W., Kostka, J. E., Gladden, J. M., Rapp, J. Z., Sharpe, J., McMahon, K. D., Treseder, K. K., Bidle, K. D., Wrighton, K. C., Thamatrakoln, K., Nusslein, K., Meredith, L. K., Ramirez, L., Buee, M., Huntemann, M., Kalyuzhnaya, M. G., Waldrop, M. P., Sullivan, M. B., Schrenk, M. O., Hess, M., Vega, M. A., O'Malley, M. A., Medina, M., Gilbert, N. E., Delherbe, N., Mason, O. U., Dijkstra, P., Chuckran, P. F., Baldrian, P., Constant, P., Stepanauskas, R., Daly, R. A., Lamendella, R., Gruninger, R. J., McKay, R. M., Hylander, S., Lebeis, S. L., Esser, S. P., Acinas, S. G., Wilhelm, S. S., Singer, S. W., Tringe, S. S., Woyke, T., Reddy, T. B. K., Bell, T. H., Mock, T., McAllister, T., Thiel, V., Denef, V. J., Liu, W.-T., Martens-Habbena, W., Allen Liu, X.-J., Cooper, Z. S., and Wang, Z. 2022. Expansion of the global RNA virome reveals diverse clades of bacteriophages. Cell 185:4023-4037.e18.

Orfanidou, C. G., Katiou, D., Papadopoulou, E., Katis, N. I., and Maliogka, V. I. 2022. A known ilarvirus is associated with a novel viral disease in pepper. Plant Pathol. 71:1901-1909.

Palanga, E., Filloux, D., Martin, D. P., Fernandez, E., Gargani, D., Ferdinand, R., Zabré, J., Bouda, Z., Neya, J. B., Sawadogo, M., Traore, O., Peterschmitt, M., and Roumagnac, P. 2016. Metagenomic-based screening and molecular characterization of cowpea-infecting viruses in Burkina Faso. PLoS One 11:e0165188.

Pallas, V., Aparicio, F., Herranz, M. C., Amari, K., Sanchez-Pina, M. A., Myrta, A., and Sanchez-Navarro, J. A. 2012. Ilarviruses of *Prunus* spp.: A continued concern for fruit trees. Phytopathology 102:1108-1120.

Parrella, G., Troiano, E., Cherchi, C., and Giordano, P. 2020. Severe outbreaks of Parietaria mottle virus in tomato in Sardinia, Southern Italy. J. Plant Pathol. 102:915-915.

Pecman, A., Adams, I., Gutiérrez-Aguirre, I., Fox, A., Boonham, N., Ravnikar, M., and Kutnjak, D. 2022. Systematic comparison of Nanopore and Illumina sequencing for the detection of plant viruses and viroids using total RNA sequencing approach. Front. Microbiol. 13:1424.

Pecman, A., Kutnjak, D., Gutiérrez-Aguirre, I., Adams, I., Fox, A., Boonham, N., and Ravnikar, M. 2017. Next generation sequencing for detection and discovery of plant viruses and viroids: Comparison of two approaches. Front. Microbiol. 8:1-10.

Poudel, B., Ho, T., Laney, A., Khadgi, A., and Tzanetakis, I. E. 2014. Epidemiology of Blackberry chlorotic ringspot virus. Plant Dis. 98:547-550.

Rai, A., Nakaya, T., Shimizu, Y., Rai, M., Nakamura, M., Suzuki, H., Saito, K., and Yamazaki, M. 2018. De novo transcriptome assembly and characterization of *Lithospermum officinale* to discover putative genes involved in specialized metabolites biosynthesis. Planta Med. 84:920-934.

Ristaino, J. B., Anderson, P. K., Bebber, D. P., Brauman, K. A., Cunniffe, N. J., Fedoroff, N. V., Finegold, C., Garrett, K. A., Gilligan, C. A., Jones, C. M., Martin, M. D., MacDonald, G. K., Neenan, P., Records, A., Schmale, D. G., Tateosian, L., and Wei, Q. 2021. The persistent threat of emerging plant disease pandemics to global food security. Proc. Natl. Acad. Sci. 118:e2022239118.

Rivarez, M. P. S., Pecman, A., Bačnik, K., Maksimović, O., Vučurović, A., Seljak, G., Mehle, N., Gutiérrez-Aguirre, I., Ravnikar, M., and Kutnjak, D. 2023. In-depth study of tomato and weed viromes reveals undiscovered plant virus diversity in an agroecosystem. Microbiome 11:60.

Rivarez, M. P. S., Vučurović, A., Mehle, N., Ravnikar, M., and Kutnjak, D. 2021. Global advances in tomato virome research: Current status and the impact of high-throughput sequencing. Front. Microbiol. 12:671925.

Roberts, J. M. K., Ireland, K. B., Tay, W. T., and Paini, D. 2018. Honey bee-assisted surveillance for early plant virus detection. Ann. Appl. Biol. 173: 285-293.

Roux, B., Rodde, N., Jardinaud, M.-F., Timmers, T., Sauviac, L., Cottret, L., Carrère, S., Sallet, E., Courcelle, E., Moreau, S., Debellé, F., Capela, D., de Carvalho-Niebel, F., Gouzy, J., Bruand, C., and Gamas, P. 2014. An integrated analysis of plant and bacterial gene expression in symbiotic root nodules using laser-capture microdissection coupled to RNA sequencing. Plant J. 77:817-837.

Rozas, J., Ferrer-Mata, A., Sánchez-DelBarrio, J. C., Guirao-Rico, S., Librado, P., Ramos-Onsins, S. E., and Sánchez-Gracia, A. 2017. DnaSP 6: DNA Sequence Polymorphism Analysis of Large Data Sets. Mol. Biol. Evol. 34:3299-3302.

Schönegger, D. 2023. Analysis of the virome and reciprocal transfers of viruses between cultivated and wild carrot populations. Ph.D. Thesis. https://theses.hal.science/tel-04033935

Sdoodee, R., and Teakle, D. 1988. Seed and pollen transmission of tobacco streak virus in tomato (*Lycopersicon esculentum* cv. Grosse Lisse). Aust. J. Agric. Res. 39:469.

Sdoodee, R., and Teakle, D. S. 1993. Studies on the mechanism of transmission of pollen-associated tobacco streak ilarvirus virus by *Thrips tabaci*. Plant Pathol. 42:88-92.

Sharman, M., Thomas, J. E., and Persley, D. M. 2015. Natural host range, thrips and seed transmission of distinct Tobacco streak virus strains in Queensland, Australia. Ann. Appl. Biol. 167:197-207.

Simkovich, A., Kohalmi, S. E., and Wang, A. 2021. Ilarviruses (*Bromoviridae*). Pages 439-446 in: Encyclopedia of Virology (Fourth Edition). D. H. Bamford and M. Zuckerman, eds. Academic Press, Oxford, U.K.

Sproviero, D., Gagliardi, S., Zucca, S., Arigoni, M., Giannini, M., Garofalo, M., Olivero, M., Dell'Orco, M., Pansarasa, O., Bernuzzi, S., Avenali, M., Cotta Ramusino, M., Diamanti, L., Minafra, B., Perini, G., Zangaglia, R., Costa, A., Ceroni, M., Perrone-Bizzozero, N. I., Calogero, R. A., and Cereda, C. 2021. Different miRNA profiles in plasma derived small and large extracellular vesicles from patients with neurodegenerative diseases. Int. J. Mol. Sci. 22:2737.

Stewart, C., Kon, T., Rojas, M., Graham, A., Martin, D., Gilbertson, R., and Roye, M. 2014. The molecular characterisation of a Sida-infecting begomovirus from Jamaica. Arch. Virol. 159:375-378.

Subramanian, S. 2016. The effects of sample size on population genomic analyses – Implications for the tests of neutrality. BMC Genomics 17:123.

Svanella-Dumas, L., Candresse, T., Lefebvre, M., Lluch, J., Valiere, S., Larignon, P., and Marais, A. 2022. First report of grapevine virus L infecting grapevine in Southeast France. Plant Dis. 106:1536.

Tauber, J. P., McMahon, D., Ryabov, E. V., Kunat, M., Ptaszyńska, A. A., and Evans, J. D. 2022. Honeybee intestines retain low yeast titers, but no bacterial mutualists, at emergence. Yeast 39:95-107.

Temple, C., Blouin, A. G., Boezen, D., Botermans, M., Durant, L., Jonghe, K. D., de Koning, P., Goedefroit, T., Minet, L., Steyer, S., Verdin, E., Zwart, M., and Massart, S. 2023. Biological characterization of an emergent virus infecting vegetables in diversified production systems: Physostegia chlorotic mottle virus. BioRxiv 535357.v2.

Temple, C., Blouin, A. G., De Jonghe, K., Foucart, Y., Botermans, M., Westenberg, M., Schoen, R., Gentit, P., Visage, M., Verdin, E., Wipf-Scheibel, C., Ziebell, H., Gaafar, Y. Z. A., Zia, A., Yan, X.-H., Richert-Pöggeler, K. R., Ulrich, R., Rivarez, M. P. S., Kutnjak, D., Vučurović, A., and Massart, S. 2022. Biological and genetic characterization of physostegia chlorotic mottle virus in Europe based on host range, location, and time. Plant Dis. 106:2797-2807.

Vannette, R. L., Mohamed, A., and Johnson, B. R. 2015. Forager bees (*Apis mellifera*) highly express immune and detoxification genes in tissues associated with nectar processing. Sci. Rep. 5:16224.

Vargas-Asencio, J., McLane, H., Bush, E., and Perry, K. L. 2013. Spinach latent virus infecting tomato in Virginia, United States. Plant Dis. 97:1663.

Verhoeven, A., Kloth, K. J., Kupczok, A., Oymans, G. H., Damen, J., Rijnsburger, K., Jiang, Z., Deelen, C., Sasidharan, R., van Zanten, M., and van der Vlugt, R. A. A. 2023. Arabidopsis latent virus 1, a comovirus widely spread in *Arabidopsis thaliana* collections. New Phytol. 237:1146-1153.

Wu, M., Kostyun, J. L., Hahn, M. W., and Moyle, L. C. 2018. Dissecting the basis of novel trait evolution in a radiation with widespread phylogenetic discordance. Mol. Ecol. 27:3301-3316.

Xu, C., Sun, X., Taylor, A., Jiao, C., Xu, Y., Cai, X., Wang, X., Ge, C., Pan, G., Wang, Q., Fei, Z., and Wang, Q. 2017. Diversity, distribution, and evolution of tomato viruses in China uncovered by small RNA sequencing. J. Virol. 91:e00173-17.

Zayed, A. A., Wainaina, J. M., Dominguez-Huerta, G., Pelletier, E., Guo, J., Mohssen, M., Tian, F., Pratama, A. A., Bolduc, B., Zablocki, O., Cronin, D., Solden, L., Delage, E., Alberti, A., Aury, J.-M., Carradec, Q., da Silva, C., Labadie, K., Poulain, J., Ruscheweyh, H.-J., Salazar, G., Shatoff, E., Bundschuh, R., Fredrick, K., Kubatko, L. S., Chaffron, S., Culley, A. I., Sunagawa, S., Kuhn, J. H., Wincker, P., Sullivan, M. B., Acinas, S. G., Babin, M., Bork, P., Boss, E., Bowler, C., Cochrane, G., de Vargas, C., Gorsky, G., Guidi, L., Grimsley, N., Hingamp, P., Iudicone, D., Jaillon, O., Kandels, S., Karp-Boss, L., Karsenti, E., Not, F., Ogata, H., Poulton, N., Pesant, S., Sardet, C., Speich, S., Stemmann, L., Sullivan, M. B., Sungawa, S., and Wincker, P. 2022. Cryptic and abundant marine viruses at the evolutionary origins of Earth's RNA virome. Science 376:156-162.